NAVAL SHIP RESEARCH AND DEVELOPMENT CENTER
Bethesda, Maryland 20034

A SEMIEMPIRICAL COMPUTERIZED METHOD FOR PREDICTING THREE-DIMENSIONAL HULL-WATER IMPACT PRESSURE DISTRIBUTIONS AND FORCES ON HIGH-PERFORMANCE HULLS

by

Robert R. Jones and Raymond G. Allen

APPROVED FOR PUBLIC RELEASE: DISTRIBUTION UNLIMITED

STRUCTURES DEPARTMENT
RESEARCH AND DEVELOPMENT REPORT

December 1972

Report 4005

A SEMIEMPIRICAL COMPUTERIZED METHOD FOR PREDICTING THREE-DIMENSIONAL HULL-WATER IMPACT PRESSURE DISTRIBUTIONS AND FORCES ON HIGH-PERFORMANCE HULLS

The Naval Ship Research and Development Center is a U. S. Navy center for laboratory effort directed at achieving improved sea and air vehicles. It was formed in March 1967 by merging the David Taylor Model Basin at Carderock, Maryland with the Marine Engineering Laboratory at Annapolis, Maryland.

Naval Ship Research and Development Center

Bethesda, Md. 20034

MAJOR NSRDC ORGANIZATIONAL COMPONENTS

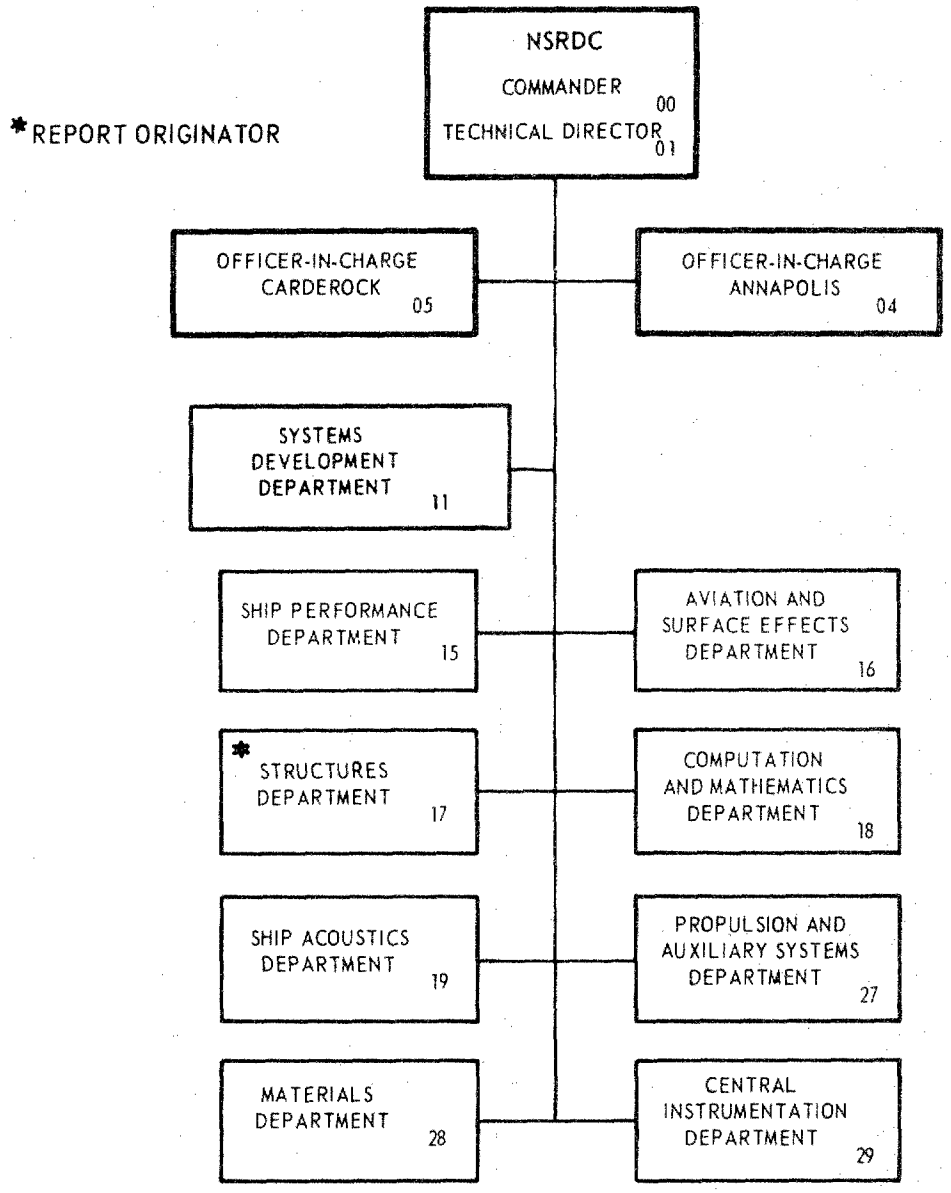

NDW-NSRDC 3960/44 (REV. 8/71)

GPO 917-872

DEPARTMENT OF THE NAVY
NAVAL SHIP RESEARCH AND DEVELOPMENT CENTER
BETHESDA, MD. 20034

A SEMIEMPIRICAL COMPUTERIZED METHOD FOR PREDICTING THREE-DIMENSIONAL HULL-WATER IMPACT PRESSURE DISTRIBUTIONS AND FORCES ON HIGH-PERFORMANCE HULLS

by

Robert R. Jones and Raymond G. Allen

December 1972

Report 4005

TABLE OF CONTENTS

LIST OF FIGURES

LIST OF TABLES

NOMENCLATURE

Symbol	Definition	Dimensions
A	Surface area	square inches
A_i	Increment of surface area for which the pressure satisfies the constraint of $P_i < P \leq P_{i+1}$	square inches
A_i'	Incremental summation of surface area for which the pressure satisfies the constraint of $P \geq P_i$	square inches
A_o	Hull impact surface area	square inches
A_T	Total load bearing hull surface area defined by a shell expansion with the chine as an outer perimeter	square inches
B	Beam	inches
C	Beam/2.0	inches
C_h	Wave propagation velocity $\sqrt{\frac{g\lambda}{2\pi}}$	inches per second
d	Distance from the hull center of gravity to the center of an incremental wedge	inches
F_v	Vertical force component of the longitudinal impact load distribution	pounds
$\dot{f}$	Equivalent planing velocity, (velocity normal to the keel)/ sin τ	inches per second
g	Gravitational acceleration	inches per second^2
k	Wave number $\frac{2\pi}{\lambda}$	per foot
L	Normal load	pounds

Symbol	Definition	Dimensions
L_i	Increment of normal load acting over the area A_i as defined by the product of $(\overline{P}_i \cdot A_i)$	pounds
L_i'	Incremental summation of normal load acting on the area A_i'	pounds
L_o	Total impact load acting everywhere normal to the impact surface area A_T	pounds
LOA	Length overall	inches
ℓ	Incremental wedge penetration depth	inches
P	Pressure	pounds per square inch
P'	Normalized pressure $\frac{P_m}{\left(\frac{1}{2} \rho V^2 \frac{1}{144}\right)}$	
P_{CALC}	Calculated pressure value using the least-squares regression curve	pounds per square inch
P_i	The i^{th} isobar pressure contour of a three-dimensional pressure distribution	pounds per square inch
$\overline{P}_i$	Average pressure defined by $\frac{P_i + P_{i+1}}{2}$ acting on the increment of surface area A_i	pounds per square inch
P_i'	True average pressure acting on the summation of incremental surface area A_i'	pounds per square inch
P_m	Maximum detected impact pressure	pounds per square inch
R	Trochoidal wave parameter as defined in Figure A.3 Residual from least-squares regression curve, $R = P - P_{CALC}$	

Symbol	Definition	Dimensions
r	Index of correlation Trochoidal wave parameter as defined in Figure A.3	
$\dot{S}$	Instantaneous velocity of hull parallel to the longitudinal centerline of the hull	inches per second
U	Incremental wedge pitch velocity	inches per second
V	Wave particle orbital velocity	inches per second
	Velocity	as noted feet or inches per second
X, Y, Z	Cartesian coordinate axes for the hull system (see Figure 5)	
$\dot{X}$, $\dot{Y}$, $\dot{Z}$	First time derivatives in the hull system	as noted inches or feet per second
X', Y', Z'	Cartesian coordinate axis for the earth system (see Figure 5)	
$\dot{X}'$, $\dot{Y}'$, $\dot{Z}'$	First time derivatives in the earth system	as noted inches or feet per second
X_m	Projection on the X axis of the total wetted length	inches
X_o	Instantaneous horizontal hull step location relative to the wave crest	inches
α	Incremental wedge trim angle relative to the hull coordinate system	degrees
β	Deadrise angle	degrees
β_{EH}	Effective horizontal deadrise angle (see Figures 3 and 4 of Reference 6)	degrees
β_{EV}	Effective vertical deadrise angle (see Figures 3 and 4 of Reference 6)	degrees

Symbol	Definition	Dimensions
θ	Hull coordinate system trim angle relative to the earth system	degrees
	Trochoidal wave parameter as defined in Figure A.3	
$\dot{\theta}$	Hull angular velocity	radians per second
λ	Wave length	inches
μ	Distance measured aft from the keel-level water surface intersection to the incremental wedge mid-section on an equivalent prismatic wedge (see Figure 2)	inches
ν	Nondimensional total wetted length of an equivalent prismatic wedge in beams (see Figure 2)	
ξ	Effective impact angle (see Figures 3 and 4 of Reference 7)	degrees
ρ	Mass density of water	slugs per feet^3
σ	Standard error of estimate	
τ	Incremental wedge trim angle relative to the water surface	degrees
ϕ	Impact angle	degrees
ω	Wave particle orbital angular velocity	radians per second

SUBSCRIPTS

CALC	Calculated
EH	Effective horizontal
EV	Effective vertical
h	Horizontal
i, k, n	Integer counter
m	Maximum

Symbol	Definition	Dimensions
o	Instantaneous or total as noted	
v	Vertical	
t	Total	

ABSTRACT

This report describes the development and usage of a semiempirical, quasi-static computerized method for calculating instantaneous three-dimensional water pressure distributions on high-speed marine vehicles. The method can simulate either planing or hull-wave impacts in three degrees of motion--pitch, heave, and surge. The analysis technique requires hull offsets, trochoidal wave parameters, and such initial condition information as the hull position, the vertical and horizontal velocity components, and the pitch rate. The method can be used to obtain results of varying complexity, including a description of normal pressures for all or selected portions of the hull, a normalized pressure versus impact area relationship, and horizontal and vertical impact forces. The results of its application to the analysis of the hull-wave impact of two model hull configurations are presented although the computer program developed for the method is not documented in this report.

ADMINSTRATIVE INFORMATION

The work presented in this report was sponsored by the Surface-Effect Ship Project Office (PM-17) under the task entitled "Load and Structural Criteria for Surface Effect Ships." Funding was provided by authorization letter, F24:MEL:et of 11 August 1971.

The report was prepared between December 1971 and June 1972. However, it is based on the results of a continuing effort over the past 2 years beginning in July 1969.

INTRODUCTION

Dynamically supported marine vehicles present a unique problem in structural design because of their high operating speeds and the not infrequent occurrence of hull-wave impacts. By nature, these vehicles are weight limited and overall structural weight must be critically examined. However, the occurrence of severe water-pressure loads demands a robust construction. Since the structural integrity cannot be jeopardized, the hull must be capable of effectively withstanding violent environmental loads yet within practical limits, its structural weight must be kept minimal.

The increasing demand for this type of vehicle emphasizes the need to establish rational design procedures that meet the competing requirements. Energy absorption capabilities must be maximized at the same time that structural weight is minimized. The result should be a general improvement in vehicle performance and capabilities.

Rational design, however, requires accurate prediction of hull-wave impacts. What is the maximum pressure developed? Where does it occur? How is the water pressure load distributed on the hull? A designer must be capable of answering these questions with confidence in order to provide a basis for rational design of the hull scantlings.

Several methods are available for determining pressure distributions during planing or during an impact.[1-3] They have had varying degrees of success in dealing with the phenomenon. However, no available method consistently produces satisfactory results nor does it attempt to deal with the entire scope of the impact problem.

The new computerized method given herein represents part of a continuing effort to produce a comprehensive design tool which eventually will deal with the entire impact phenomenon, from initial impact to resultant trajectories and structural response. The method of analysis is based on suggestions by Gray et al.[4] and Jenson.[2]

According to those suggestions, the hull is approximated by a series of V-bottom prismatic wedge increments whose physical dimensions are determined by the hull geometry. The pressure distribution on each slice is

---

[1]Chey, Y. H., "Hull-Wave Impact Load on High-Speed Marine Craft," Stevens Institute of Technology, Davidson Laboratory Report 1072 (May 1965).

[2]Jensen, W. R., "Hydrofoil Boat Hull-Wave Impact Loads," Grumman Aircraft Engineering Corporation Report GE-173 (Aug 1959).

[3]Chuang, S. L., "Pressure Distributions on Wedge-Shaped Hull Bottoms of Hydrofoil Craft during Crash Landings," NSRDC Report 2953 (Aug 1969).

[4]Gray, H. P. et al., "Prediction of Three-Dimensional Pressure Distributions on V-Shaped Prismatic Wedges during Impact or Planing," NSRDC Report 3795 (Feb 1972).

calculated as if the whole hull were composed of that particular wedge shape.[4] Relevant portions of these various distributions are then synthesized to obtain the final, "realistic" pressure distribution.

The method is capable of obtaining pressure distributions on any specified hull shape. Pure planing or hull-wave impacts in idealized wave forms can be simulated for three degrees of motion--pitch, heave, and surge. Computer output includes a full or partial pressure distribution, horizontal and vertical impact forces, and normalized pressure and load versus impact area relationships.

The capabilities of the computerized method are demonstrated by its application to two hull forms, one a model with varying deadrise and the other a model with constant deadrise. The operating conditions were identical with the experimental parameters presented by Chey.[1] Results obtained from the analysis are compared with the Chey experimental data and theoretical predictions.

MODELING TECHNIQUE

Theories developed to explain the impact phenomenon are based primarily on the behavior of the V-shaped prismatic wedge during liquid impact. Historically, this analysis technique finds its roots in the early investigations of seaplane landing impacts. The V-shaped body was not only fairly typical of the cross section of seaplane hulls but was also conducive to mathematical modeling techniques. It was comparatively easy to analyze, and it provided a simple shape from which data could easily be obtained. Further, it furnished a numerical basis for predicting the behavior of the cross sections of more complex hulls.

In this report, the modeling technique is likewise based on prismatic wedge theory. It extends the work of Gray et al.[4] in an attempt to more closely approximate realistic hull shapes, and it includes modifications that facilitate programming and produce results which improve the correlation with experimental data.

The method consists of dividing the hull into incremental wedge portions which are defined by the offsets of the keel and chine in both the plan and profile views. A typical model is shown in Figure 1. The numbering system and coordinates indicated in Figure 1 are used throughout this

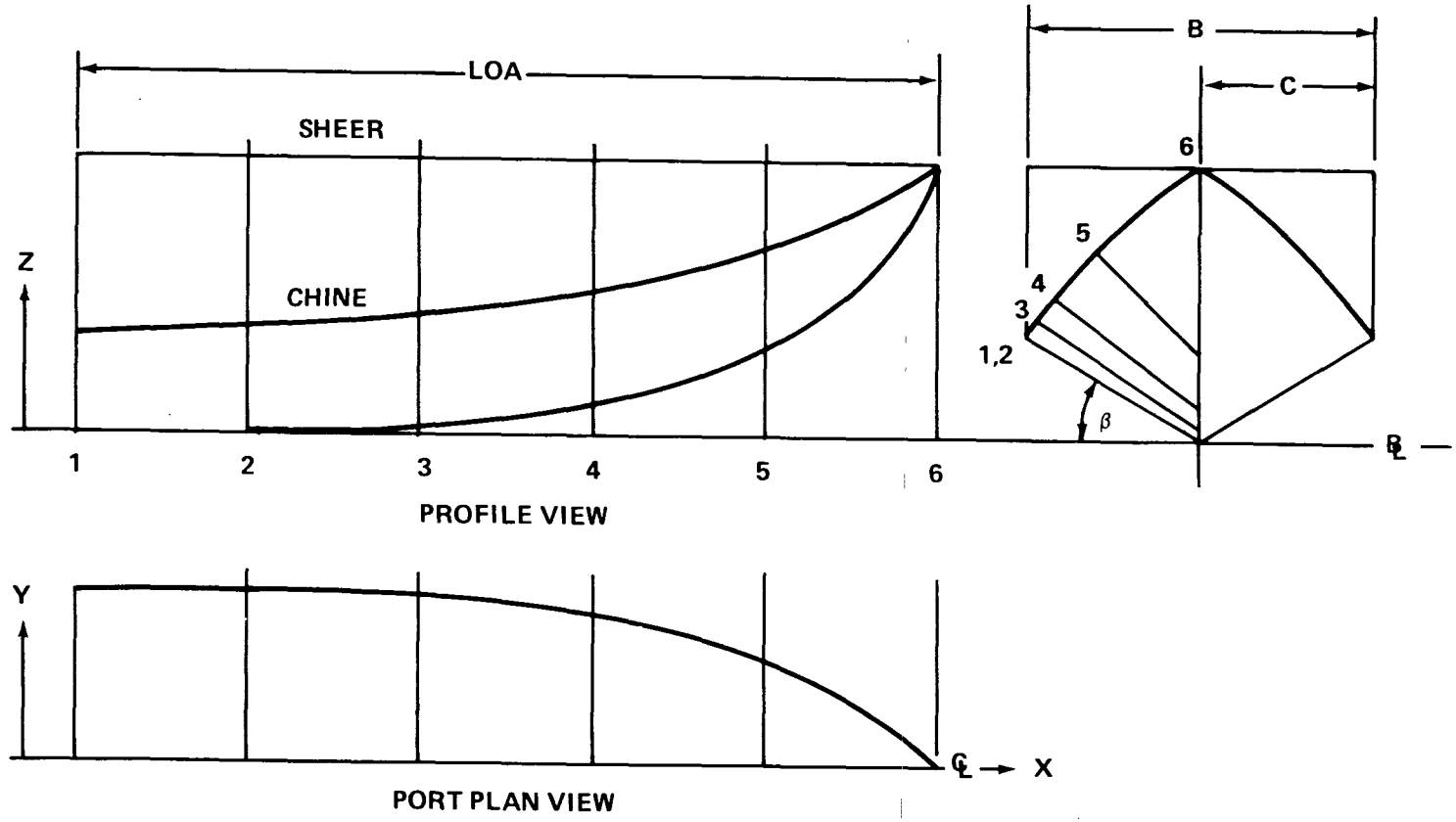

Figure 1 - Typical High-Performance Hull

report and in the computer program. Each incremental wedge is assumed to be part of a longer, V-bottom prismatic wedge which has the same trim τ, deadrise angle β, and beam B.

The total wetted length of the equivalent prismatic wedge μ is calculated according to the following scheme. The elongated, equivalent wedge is defined so that the relative longitudinal position of the wedge increment ν is the same on both the elongated wedge and the hull; see Figures 2 and 3. Additionally, the wedge increment must have the same penetration depth ℓ.

Once the trim, deadrise angle, beam, and wetted length of each elongated prismatic wedge are defined, the corresponding centerline pressure distribution is calculated. This is accomplished by assuming that the entire hull is composed of that particular wedge shape and using the method described by Gray et al.[4] The portion of this distribution which maintains the same relative longitudinal hull position as that of the original wedge increment is assumed to be the pressure distribution over that wedge on the hull. Figure 3 demonstrates this procedure for one incremental wedge. The relevant incremental portions of the centerline distribution are synthesized to produce the distribution for the realistic hull as shown in Figure 4.

Transverse distributions are calculated at the aft, center, and forward sections of the incremental wedges. The magnitudes depend on the derived centerline distribution, and the transverse trends are determined by wet or dry-chine location. Generally speaking, wet-chine transverse distributions tend to decrease in magnitude from centerline to chine. Dry-chine transverse distributions display the opposite tendency.

When all wedges are synthesized, the end result is a three-dimensional representation of the distribution of pressure on the hull. The same procedure is followed for both pure planing and hull-wave impacts.

The above procedure deals only in values which are normalized against their own local maximum pressures, as in Gray et al.[4] In order to develop quantitative magnitudes for the pressure distribution, the maximum values of pressure must be evaluated at the location of each transverse distribution. The process utilized for determining maximum pressures is examined in the following section.

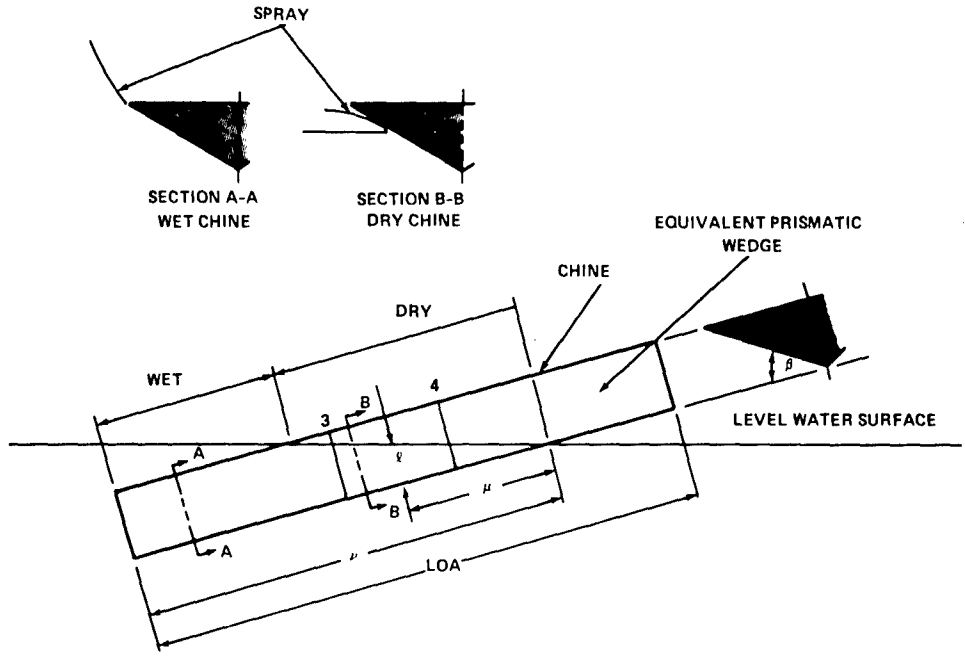

Figure 2 - Geometry of an Equivalent Prismatic Wedge

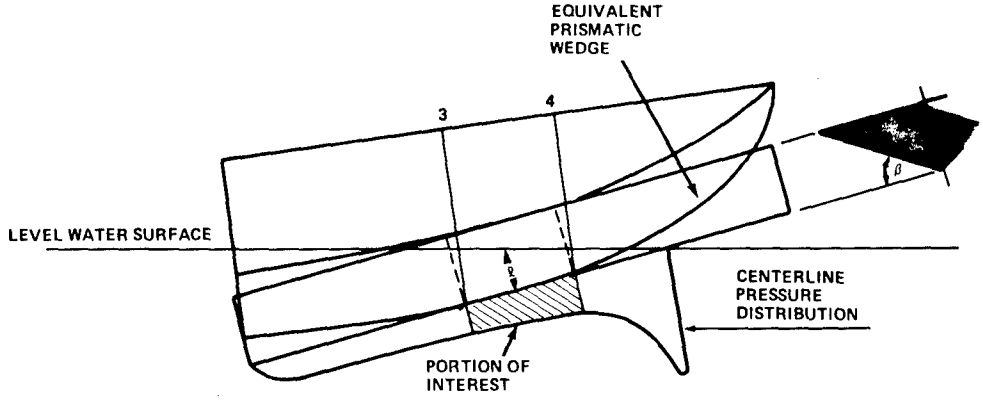

Figure 3 - Centerline Pressure Distribution for One Incremental Prismatic Wedge on a Typical Hull

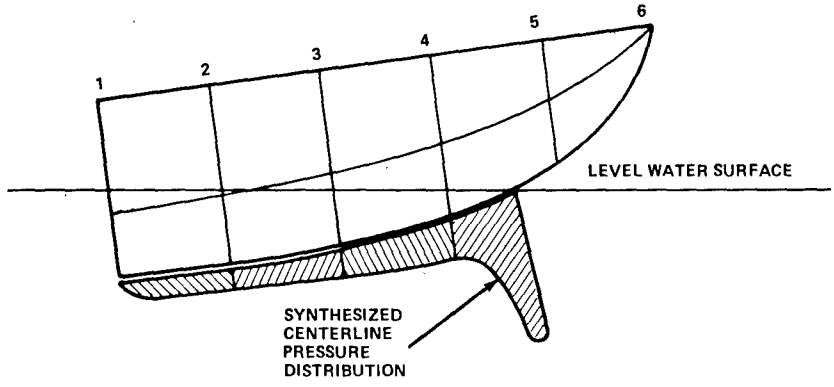

Figure 4 - Synthesized Centerline Pressure Distribution on a Typical Hull

DETERMINATION OF THE MAXIMUM IMPACT PRESSURE

The normalized three-dimensional pressure distributions developed for each section of the realistic hull lack meaning unless maximum impact pressure values P_m are defined locally. Incremental wedge modeling requires that P_m be developed for each transverse distribution because of variations in controlling and contributing velocity parameters. For the special cases of calm water planing or impacting, this requirement is relaxed and P_m values are required only for each incremental wedge. However, there is still the problem of how to calculate P_m.

The discussion by Gray et al.[4] for calculating P_m is based on work by Smiley.[5] Smiley contended that, with certain exceptions, the impact pressure distribution on a wedge was qualitatively the same as the planing pressure distribution. That is, the shape of the pressure distribution over the wetted surface area is essentially the same for either the planing or impacting prismatic body, provided that the geometric conditions of trim, deadrise, and wetted length to beam ratio are constant. Quantitatively, however, they differ. For the case of pure planing, the maximum pressure is a function of only the horizontal planing velocity. Maximum impact pressures, on the other hand, are a function of a derivative of both the horizontal and vertical velocities. This distinction is explained further below.

According to Smiley,[5] P_m may be found from

$$P_m = 1/2\ \rho\ \dot{f}^2 \qquad (1)$$

---

[5]Smiley, R. F., "A Semiempirical Procedure for Computing the Water Pressure Distribution on Flat and V-Bottom Prismatic Surfaces during Impact or Planing," National Advisory Committee for Aeronautics TN 2583 (Dec 1951).

where ρ is the mass density of water and f is the equivalent planing velocity (the speed of advance of the spray root parallel to the water surface). A vectorial derivation of $\dot{f}$ is shown in Figure 5, and it is defined as

$$\dot{f} = \dot{X}' + \dot{Z}' \cot \tau = \frac{\dot{Z}}{\sin \tau} \tag{2}$$

where $\dot{X}'$ is the total horizontal velocity component,

$\dot{Z}'$ is the total vertical velocity component,

$\dot{Z}$ is the velocity normal to the keel, and

τ is the incremental wedge trim angle relative to the water surface.

Since, in general, P_m must be defined for each location of a transverse pressure distribution, so must $\dot{X}'$ and $\dot{Z}'$. They are defined as

$$\dot{X}' = U_h + V_h + W_h \tag{3}$$

and

$$\dot{Z}' = U_v + V_v + W_v \tag{4}$$

where V is the velocity of the hull,

W is the wave particle orbital velocity, and

U is the incremental wedge pitch velocity.

The subscripts h and v indicate horizontal and vertical velocity components, respectively. The incremental wedge pitch velocity is further defined by

$$U_h = d \dot{\theta} \sin \tau$$

and

$$U_v = d \dot{\theta} \cos \tau$$

where d is the distance from the hull center of gravity to the center of the incremental wedge,

$\dot{\theta}$ is the pitch velocity in radians per second, and

τ is the incremental wedge trim angle measured in degrees.

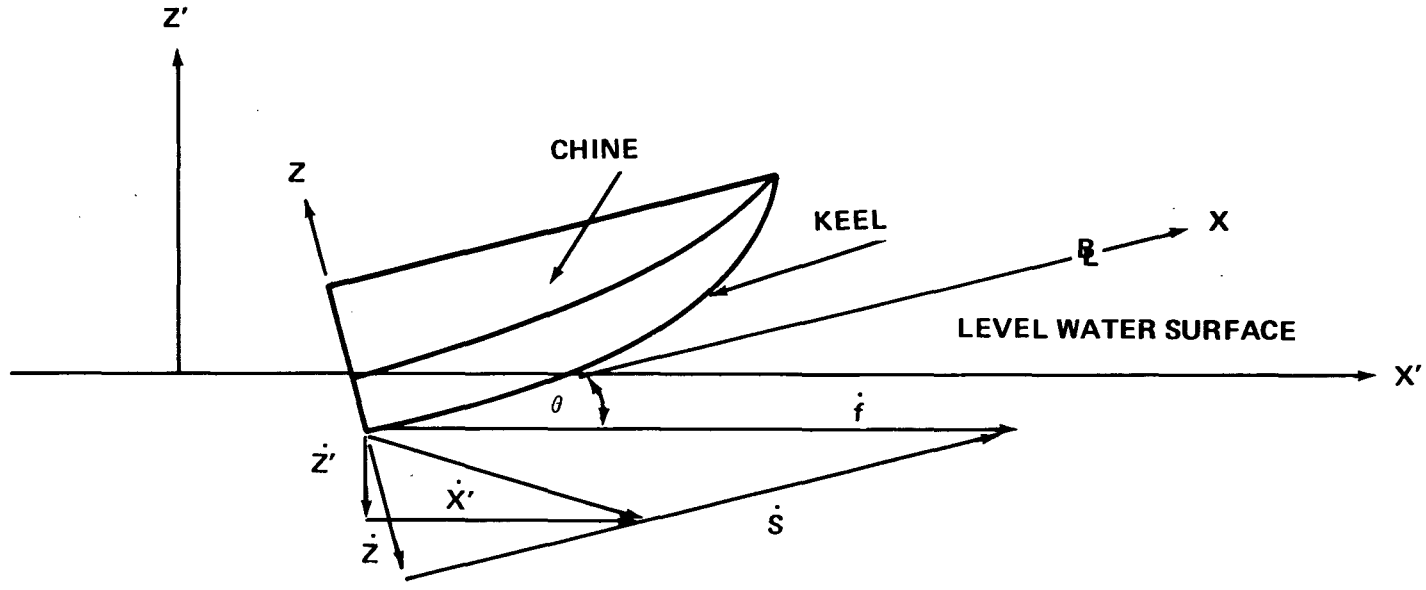

Figure 5 - Vectoral Derivation of the Equivalent Planing Velocity $\dot{f}$

The components of W are found by using an approximation for the standard trochoidal wave, which is further described in Appendix A.

Figure 6 indicates the directions of motion and sources of the various velocity components. The term C_H is included as a component of the total horizontal velocity. It represents the wave propagation velocity for a harmonic deep-water wave

$$C_H = \sqrt{g \frac{\lambda}{2\pi}} \tag{5}$$

where g is the acceleration due to gravity and λ is the wave length. Although this component is used by Chuang,[6] the physical interpretation is a subject for more experimental investigation. Further discussion concerning this velocity component is given in the sample problem.

For examples of pure planing, Equation (2) reduces to $\dot{f} = \dot{X}'$. The planing pressure distribution is, then, proportional to the square of the planing velocity $\dot{X}'$.

For examples that include vertical impact velocities, $\dot{Z}' > 0.0$, however, the behavior is rather different than indicated by classical theory. According to Equation (2), for trim angles approaching 0 deg, the speed of advance of the spray root parallel to the water surface $\dot{f}$ approaches infinity. Subsequently, the maximum pressure P_m becomes infinite. Experimental evidence does not indicate that this is true.

Chuang has experimentally investigated impacts for two-dimensional wedges and three-dimensional cones with deadrise angles of 15 deg and less. He has demonstrated that classical theories fail at small deadrise angles due to the presence of trapped air. Chuang and Milne[7] have summarized the empirically derived formulas for determining maximum impact pressure. The

---

[6]Chuang, S. L., "Design Criteria for Hydrofoil Hull Bottom Plating (A Practical Application of Research on Slamming)," NSRDC Report 3509 (Jan 1971).

[7]Chuang, S. L. and D. T. Milne, "Drop Tests of Cones to Investigate the Three-Dimensional Effect of Slamming," NSRDC Report 3543 (Apr 1971).

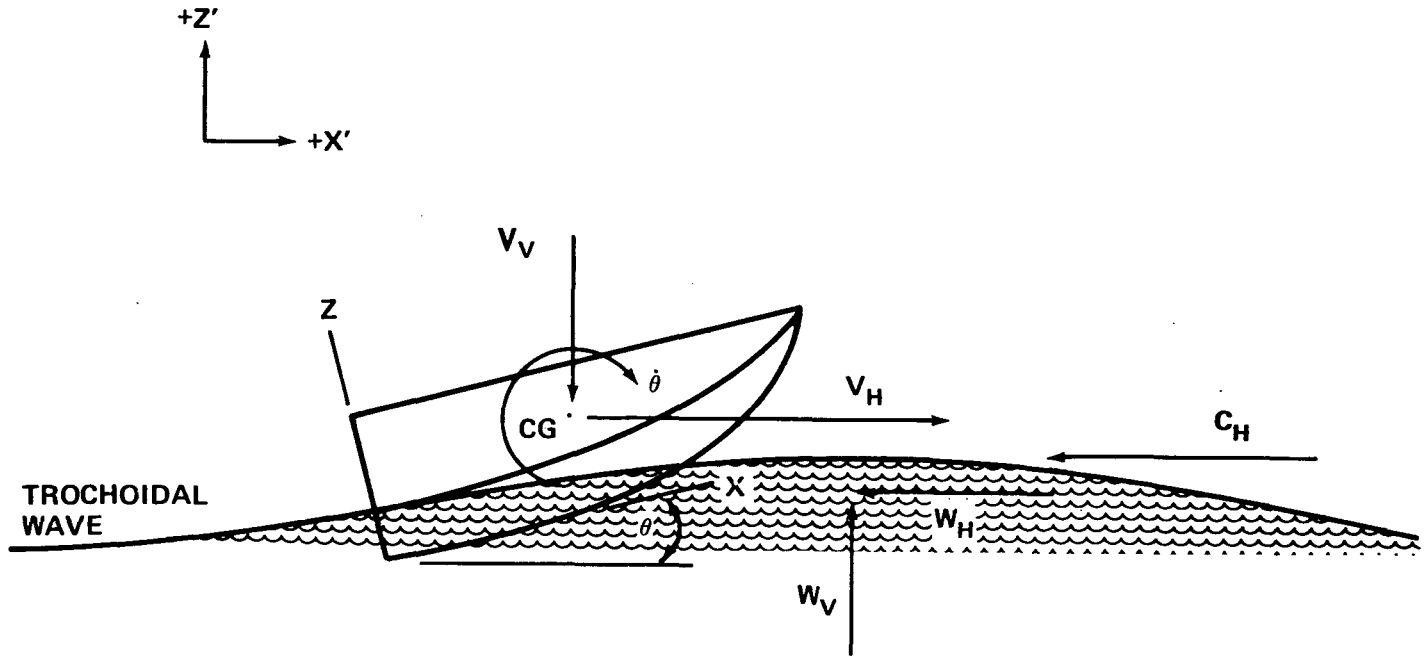

Figure 6 - Representation of the Various Components for the Horizontal and Vertical Velocities

equations indicate that for low deadrise angles, P_m does not behave as Equation (1) dictates. Instead, P_m values at the keel peak out at a deadrise of 1.0 deg and then fall off for $\beta = 0.0$ deg. Chuang has attributed this behavior to the presence of trapped air which, in effect, decreases the mass density ρ locally at the impact surface.

Intuitively, the behavior of Equation (2), which ascribes an infinite value to the spray root velocity, is not legitimate for low trim angles. The velocity must have some absolute maximum, finite value. For this reason, the empirical equations in Chuang and Milne[7] have been incorporated to correct the inherent deficiencies of Equation (2). The assumptions necessary to relate β and τ are discussed in Appendix B.

The impact is classified as one of two possible types: (1) a purely vertical component and (2) a combination of vertical and horizontal velocity components.

During a vertical impact where $\dot{X}' = 0.0$ and $\dot{Z}' > 0.0$, P_m is determined by using the Chuang empirical equations for the vertical impact of a two-dimensional wedge.[6,7] The extent to which this deviates from Equations (1) and (2) will be discussed in Appendix B.

For any other type of impact where $\dot{X}' > 0.0$ and $\dot{Z}' > 0.0$, a tradeoff is used. It is based on Equation (2), and the aforementioned empirical equations[7] for three-dimensional cones and circular plates. The tradeoff is also discussed in Appendix B.

Normalized versions of these two curves are presented in Figure 7. They are used to evaluate the maximum impact pressure and are dependent on the type of impact. The term P' is introduced here as

$$P' = P_m / \frac{1}{2} \rho V^2 \frac{1}{144} \tag{6}$$

and it is used as the ordinate of Figure 7. The maximum pressure P_m in pounds per square inch is found by using Equation (6) and Figure 7 with the following substitutions:

1. Vertical impact, $\dot{X}' = 0.0$, $\dot{Z}' > 0.0$: $V = \dot{Z}'$ (in feet per second) and $\phi = \xi$ (in degrees).

2. Vertical and horizontal impact, $\dot{X}' > 0.0$, $\dot{Z}' > 0.0$: $V = \dot{Z}$ (in feet per second) and $\phi = \tau$ (in degrees).

Where ρ is the mass density, slugs per foot^3

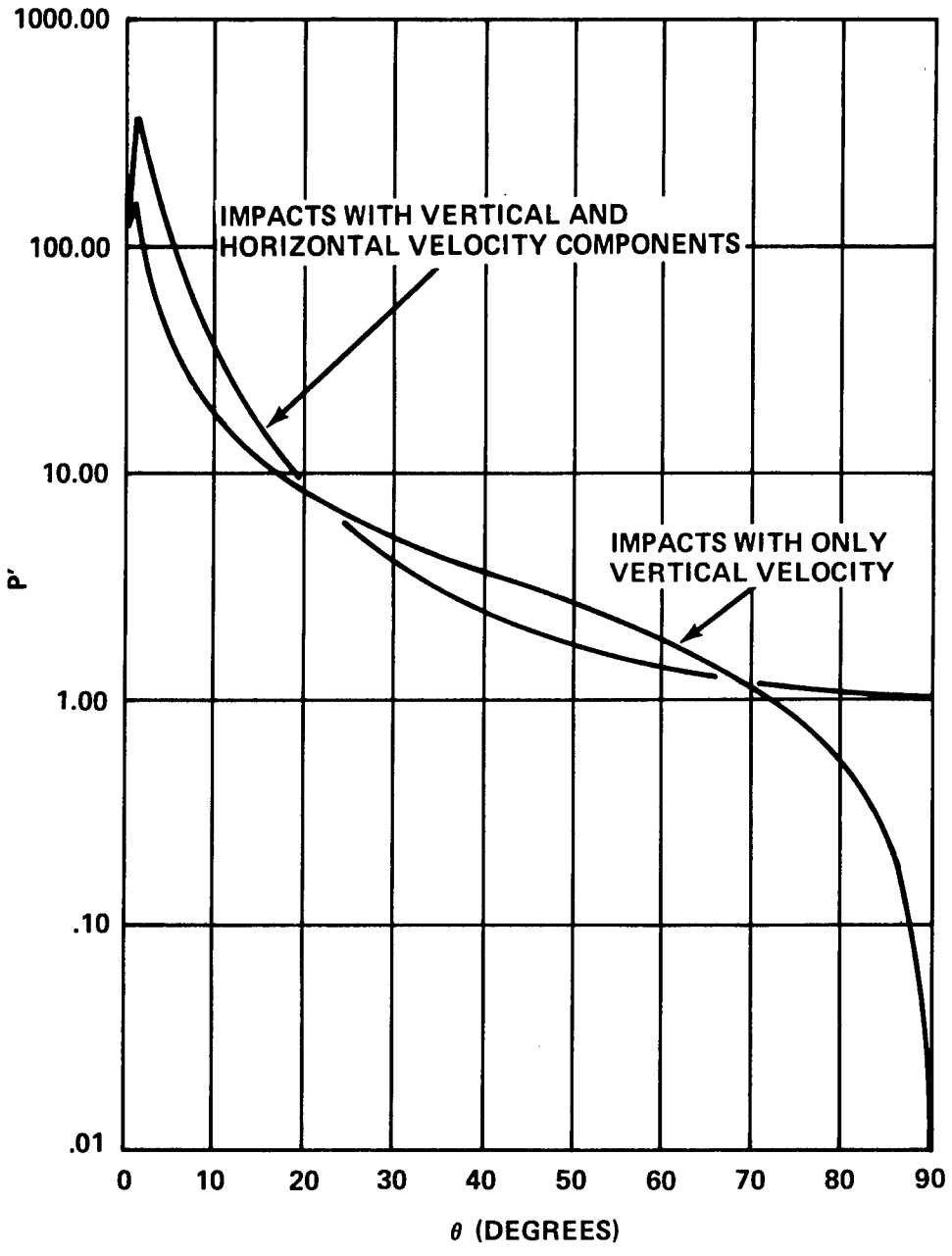

Figure 7 - Normalized Curves for Determining Maximum Impact Pressures

$$\tan \xi = \cos \beta_{EH} \tan \tau + \sin \beta_{EH} \tan \beta_{EV}$$

$$\beta_{EH} = \tan^{-1} (\tan \beta / \sin \tau) \qquad (7)$$

$$\beta_{EV} = \tan^{-1} (\tan \beta / \cos \tau)$$

The total effective deadrise angle ξ and the respective horizontal and vertical effective deadrise angles β_{EH} and β_{EV} are from Chuang.[6] Derivations for ξ, β_{EH}, and β_{EV} are also given by Chuang.[6]

The above process is used to calculate P_m at each location of a normalized transverse pressure distribution. The product of $P_m \cdot P/P_m$ at each location results in the actual three-dimensional pressure distribution for the modeled hull.

ANALYSIS OF PRESSURE AND LOAD VERSUS IMPACT AREA

Each occurrence of a hull-water impact is a unique event. As has been shown, the magnitude and the shape of the resulting pressure distribution depend on several parameters. The most important of these parameters--the trim, the deadrise, and the velocity components--dictate the severity of the impact. During its operational lifetime, a hull will be subjected to countless variations of these dominant parameters. Likewise, all the descriptive characteristics of the impact, such as the peak pressure, the impact area, and the shape of the distribution, will have countless variations.

From a design standpoint, there is need for something more than just the three-dimensional pressure distribution, e.g., a method which, ideally, can minimize the uniqueness and provide a more thorough description of the impact phenomenon. Toward this end, two methods of integrating the pressure surface are included in the analysis technique. The first is relatively simple in nature and requires only minor discussion, but the second demands a more complete explanation.

The first method is based on the incremental wedge modeling technique and trapezoidal integration. For each wedge, there are three transverse pressure distributions. They define a "volume" of pressure which is acting

normal to the surface area of the wedge. The magnitude of this volume is merely an incremental portion of the total impact load. The longitudinal distribution of the impact load normal to the keel is determined by calculating the "volume" for each wedge and by assuming symmetric impact in the transverse direction. Since each incremental wedge may have a different effective trim angle, the horizontal and vertical components of the normal load must be calculated on each wedge. The summation of the component forces gives the total horizontal and vertical impact forces.

Two points should be noted regarding the longitudinal distribution of forces. First, as mentioned, the distribution is assumed to act at the keel since only symmetric bow impact is considered and the pressure "volumes" on either side of the keel are identical. Second, in the longitudinal direction, the point load for each incremental wedge is assumed to act at the wedge midpoint. In general, this is not exactly the case. However, the proper choice of wedge sizes minimizes any deficiency of this assumption.

The second integration technique may be called isobaric or contour integration. It was developed in an effort to establish the actual relationships between the pressure and load distributions versus the hull impact area. This approach is based on one of the basic characteristics of the impact phenomenon on a prismatic wedge. Generally speaking, the maximum detected pressures act over relatively small areas of the hull surface. As a result, the portion of the total impact load which is represented by high pressure areas is also small. Conversely, lower pressures are evident over a greater portion of the impact area, and they represent a higher percentage of the total load. This concept may be thought of in a normalized form of pressure P/P_m, load L/L_o, and area A/A_o ratios. Here P/P_m is the pressure ratio based on the maximum detected pressure P_m acting everywhere normal to the impact surface area, L/L_o is the load ratio based on the total load L_o acting everywhere normal to the impact surface area, and A/A_o is the area ratio based on the hull impact surface area A_o. The pressure ratio P/P_m is a monotonically decreasing function of the area ratio A/A_o. On the other hand, the load ratio L/L_o is a monotonically increasing function of the area ratio A/A_o.

Now in order to generate the mathematical relationship between the pressure, the load, and the area, we let P_i represent the i^{th} isobar

pressure contour of the three-dimensional pressure distribution. It is used to define two areas A_i and A_i'. A_i designates the area for which the pressure P is

$$P_i < P \leq P_{i+1} \tag{8}$$

This is an exclusive area since the pressure must satisfy an upper and lower limit. Consequently, A_i also defines an incremental load L_i representative of the average pressure $\overline{P}_i$ acting on A_i, where

$$L_i = \overline{P}_i A_i \tag{9}$$

and $\overline{P}_i$ is defined for analysis purposes as

$$\overline{P}_i = \frac{P_i + P_{i+1}}{2} \tag{10}$$

On the other hand, A_i' must satisfy only the constraint that

$$P \geq P_i \tag{11}$$

A_i' is not an exclusive area since it may be composed of several discrete A_i's. As such, the A_i areas must satisfy the relationship

$$A_i' = \sum_{k=i}^{n} A_k \tag{12}$$

Finally, the incremental load L_i' acting on the area A_i' is calculated by

$$L_i' = \sum_{k=i}^{n} L_k \tag{13}$$

This provides sufficient information to develop the true average pressure acting over the area A_i', or

$$P_i' = \frac{L_i'}{A_i'} \tag{14}$$

This operation must be performed for several discrete values of P_i over the range of $0 \leq P_i \leq P_m$. Likewise, L_i' and P_i' must also be defined for each P_i. The process accounts for the effects of distributed pressures and loading over a given surface area, and it develops the functional relationships between the pressure, the load, and the area.

Figure 8 demonstrates the general trends of these relationships. The curves shown are characteristic of those developed for a hull composed of prismatic wedges with varying deadrise angles. The value of P/P_m at $A/A_o = 1.0$ may be interpreted as the average normalized pressure which is everywhere normal to the entire impact surface area A_o.

The limited number of cases analyzed according to this method indicate that a generalization such as shown in Figure 8 may be justified for cases where the deadrise angle is greater than zero. As expected, flat bottom surfaces may demonstrate very different characteristic tendencies than those shown in Figure 8 for the prismatic wedges. Further discussion of this point is given in Appendix C and in the sample problem.

Appendix C is included to demonstrate the contour integration method and to provide a design application of the method to an idealized model.

DESCRIPTION OF THE COMPUTER PROGRAM

Computer program IPPRES is written in FORTRAN IV for use on the CDC 6700 computer at NSRDC. Using the procedures discussed in earlier sections and the computer program of Gray et al.,[4] IPPRES is capable of predicting pressure distributions for bow-symmetric hull-water impacts. It is composed of numerous distinct subroutines which are responsible for various portions of the impact analysis. The subroutine program format was chosen to allow for rapid adaptation of improved empirical analysis techniques and for ready incorporation of additional data on the impact phenomenon.

The mathematical description of the hull is provided by a table of offsets and/or by plan and profile drawings. Idiosyncracies of the program

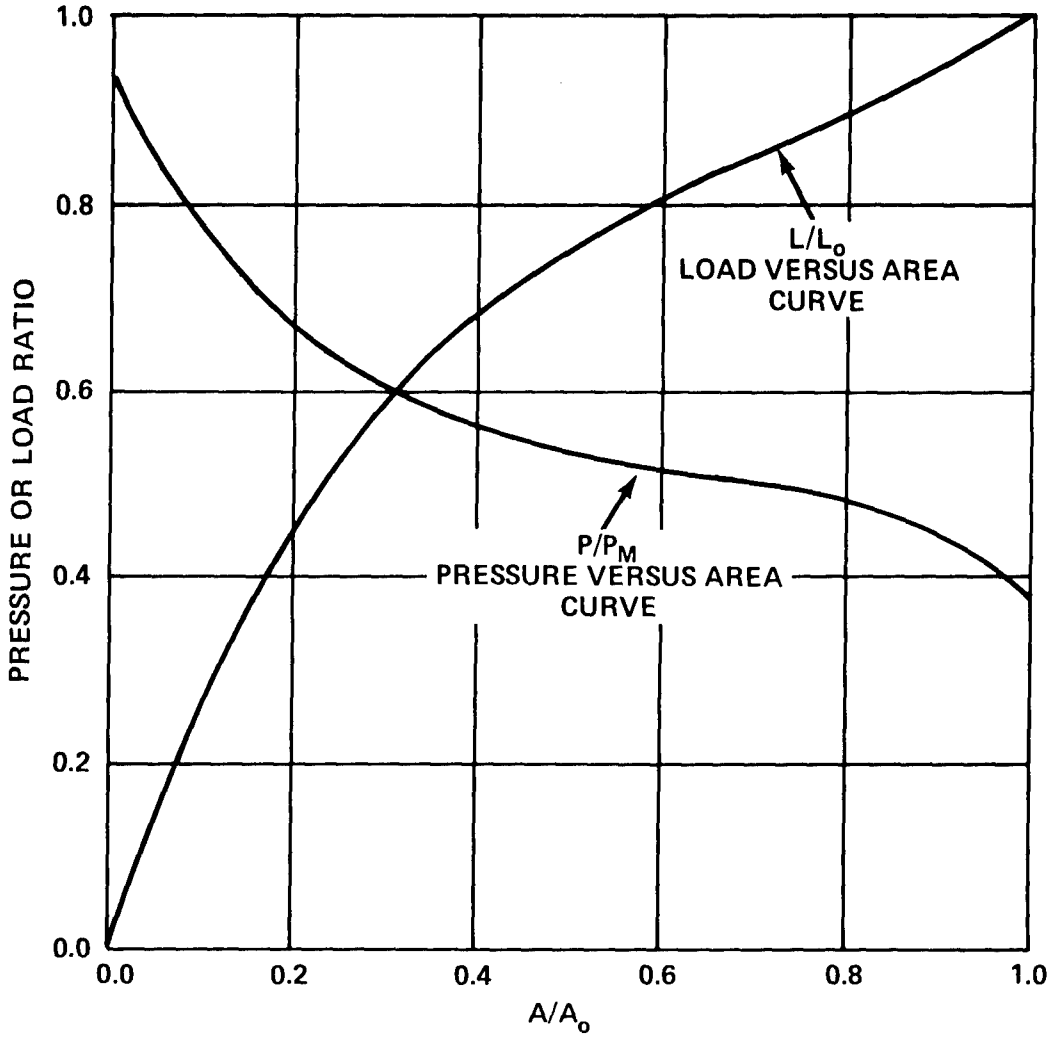

Figure 8 - Typical Normalized Pressure and Load versus Impact Area Relationship

and past experience both indicate that station spacing should be in the neighborhood of 0.05 LOA. Offsets are needed only for the keel and chine (in the X, Y, Z coordinates) in order to define the hull as a series of prismatic wedges. The offsets may require slight modifications to ensure fairness of the hull. Figure 9 shows one of the series of wedges; the deadrise, trim, and beam are assumed to be constant between adjacent stations n and n + 1. Figure 9 also indicates that the freeboard is assumed as vertical from chine to sheer.

Variations from the hard-chine hull of Figure 9 demand either additional assumptions or increased modeling complexity. The soft-chine cross section of Figure 10 may be adequately, but conservatively, modeled by assuming a hard chine. As shown, it is based on a tangent line at the point of minimum deadrise. Although areas farther away from the keel should indicate higher than normal pressures, the more important low deadrise area near the keel will be precise.

The flair-bow section of Figure 11 may be handled in one of two ways. First, it may be "roughly" approximated by an equivalent wedge section as shown in Figure 11a. Here, it has been modeled as the computer program would, assuming a straight line from keel to chine. However, provided the beam is held constant, a corrected chine may be chosen (also shown in Figure 11a) to use a more appropriate deadrise angle. The computer modeled wedge of Figure 11 would result in higher than normal pressures near the keel and lower than normal pressures away from the keel. The corrected chine model would also give higher than normal pressures at the keel, but would be more representative of pressures in the near-chine region.

Secondly, as shown in Figure 11b, the flair bow may be modeled by using partial wedges. In this case equal portions of the flair section are simulated by four wedges of different deadrise angles but similar beams. Partial Wedge 1, indicated by line A-A and the centerline, models the section from centerline to Buttock 1, and so on. The final pressure distribution is found by summing the parts. This approach is justifiable for simple hulls or where accurate modeling is required. In most instances, however, the modeling of Figure 11a is sufficient.

Once the hull is mathematically defined, it is rotated and translated into the earth (or water) coordinate system. For calm water planing

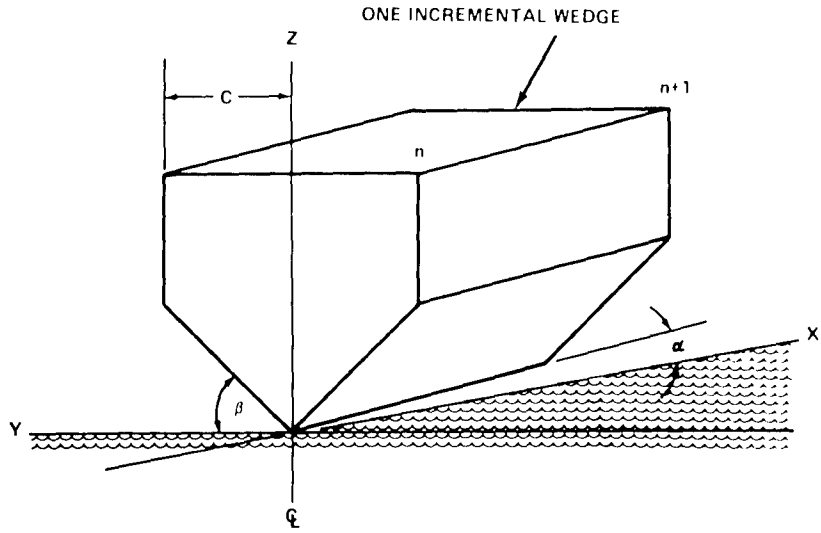

Figure 9 - Modeling Geometry for a Typical Incremental Wedge

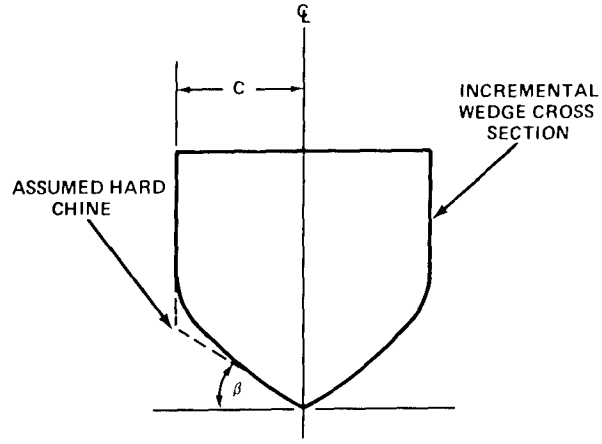

Figure 10 - Suggested Modeling Geometry for an Incremental Wedge with a Soft-Chine Section

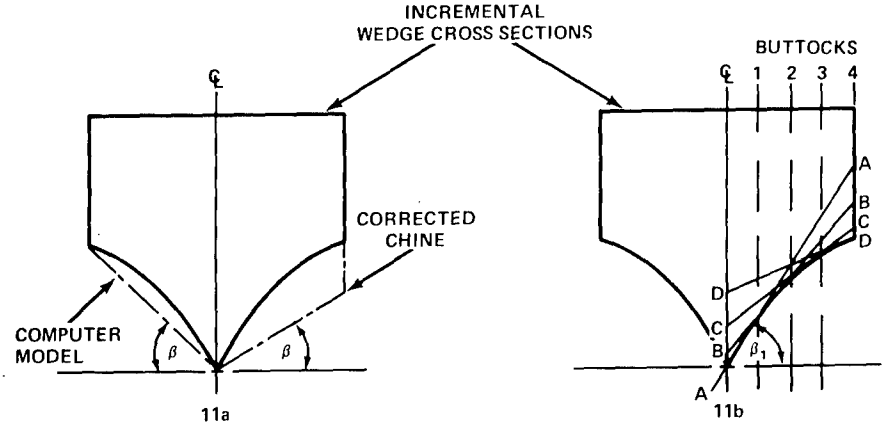

Figure 11 - Suggested Modeling Geometry for an Incremental Wedge with a Flair Section

or impact, the horizontal location is immaterial; only the vertical step location influences the pressure magnitudes. Instances of hull-wave impacts are greatly influenced by both the vertical and horizontal location of the step with regard to wave crests and the mean waterline. Correct placement of the hull in the water is necessary in order to calculate penetration depths for each station. Wedge penetration depths are defined as the average of the wedge boundary station penetration depths.

As described in the section on modeling technique, the equivalent prismatic wedges are mathematically formulated by using the beams, deadrise angles, trim angles, and penetration depths for each incremental wedge. The computer program by Gray et al.[4] is used to calculate the normalized water pressure distribution at the boundary stations and midpoint of each incremental wedge. This is accomplished in two sections. First, the centerline distribution is calculated. Second, the wedge is defined as either wet or dry chine by comparing the penetration depth to the Z-coordinate of the chine. The proper transverse distribution is then calculated.

The above process is repeated for each equivalent wedge. Then, the relevant portions of the wedge pressure distributions are synthesized to approximate the distribution on the modeled hull. The result is a normalized pressure distribution of P/P_m values, where P_m is unique for each station.

The velocity input data are used to classify the impact as purely vertical or as a combination of vertical and horizontal velocity components. Maximum pressure values P_m are defined according to the classification summarized in Figure 7. The process is repeated for each station, and the result is multiplied by its normalized counterpart to obtain the true magnitude of the pressure distribution.

The longitudinal distribution of horizontal and vertical forces is determined by using the incremental wedge pressure distributions. Trapezoidal integration is used to determine the area enclosed by each of the three transverse pressure distributions. An average of the three is taken, and it is assumed to represent the typical distribution for that wedge. This averaging process is part of the reason for specifying a maximum distance on station spacing. Stations closer than 0.05 LOA would provide

more accurate results. However, computer time increases asymptotically and thus becomes prohibitive. The impact force is obtained by multiplying the typical transverse pressure section by the length of the incremental wedge. The force is normal to the keel and acts at the center of the wedge, as explained in the section on determination of impact load.

The pressure distribution is also numerically integrated according to the isobaric contour technique. It describes the behavior of the impact pressure and load versus the impact area. For this type of integration, the load is assumed to act everywhere normal to the hull. As such, it is related to the vertical component of the longitudinal load distribution by the cosine of the trim τ and deadrise β of each incremental wedge, or

$$L_o \sim \sum_{i=1}^{k} (F_v)_i / \cos \beta_i \cos \tau_i \qquad (15)$$

where L_o is the total impact load acting everywhere normal to the impact surface area and $(F_v)_i$ is the vertical force component of the longitudinal impact load distribution acting on wedge i. Programming techniques utilized in the two different integration routines indicate that a solution of Equation (15) will result in a discrepancy of approximately 4 percent. In addition, the isobaric integration subroutine provides information for the maximum detected pressure within the pressure distribution and the hull impact surface area.

The entire computerized method is based on an instantaneous analysis of the impact phenomenon. In this respect, it demands prior knowledge of the trim, velocity components, and location of the hull in a wave profile. This "static" approach may be transformed into a quasi-static analysis by knowing, or assuming, time histories for the above three parameters. Such an approach is given in the sample problem.

INPUT DATA PREPARATION

The following data cards must be prepared according to their respective formats. All units are in inches, pounds, and seconds.

CARD 1 - Format (I10, 4X, 10A6)

LAST — The number of different hull operating conditions to be simulated.

ATITLE — Columns 15-75 are available for a title which is printed out on the first page of output.

CARD 2 - Format (2I10, 2F10.4)

N — The number of stations used to define the hull geometry. N must be $\leq$ 51.

IMCL — The option that controls the manner in which the incremental wedge trim angles are calculated. If IMCL = 1, the wedge trim angles will be calculated from the "mean-chine line" whose Z-coordinates must be fed in at each X-offset (see Card 5). If IMCL > 1, the wedge trim angle will be calculated by using the keel Z-offsets, and Card 5 may be omitted.

CØNV — The conversion factor used to relate digitized data units to inches. If the input data are not digitized, make CØNV = 1.0.

VNØC — The conversion factor used to relate the model drawing scale to actual size in inches. If no scale is used, make VNØC = 1.0.

CARD 3 - Format (F10.4); see Figure 12

XSTERN — The X-coordinate of the hull step in the hull coordinate system in inches if CØNV = VNØC = 1.0. For most cases, XSTERN = 0.0.

CARD 4 - Format (5F9.0); see Figure 12

XKEEL — The X-coordinate of the keel at each station.

YKEEL — The Y-coordinate of the keel at each station. For most cases, YKEEL = 0.0.

YCHINE — The Y-coordinate of the chine at each station.

ZKEEL — The Z-coordinate of the keel at each station.

ZCHINE — The Z-coordinate of the chine at each station. Card 4 must be repeated for each of the N hull stations, beginning at the step. If CØNV = VNØC = 1.0, the above coordinates must be in inches. YCHINE - YKEEL $\neq$ 0.

CARD 5 - Format (8F9.0); see Figure 12

ZMNCHL — The Z-coordinate of the "mean-chine line" at each X-offset station in inches if CØNV = VNØC = 1.0. Card 5 is present only if IMCL = 1; otherwise omit it and continue to Card 6. Card 5 must be repeated a sufficient number of times to feed in the N values of ZMNCHL. A detailed explanation of the mean-chine line is given in the sample problem.

CARD 6 - Format (2I10, F10.4, 2I10)

ICASE — The arbitrary individual case reference number.

IRHØ — The fresh or salt water density option. If IRHØ = 1, fresh water density will be used. If IRHØ = 2, salt water density will be used.

TRIMD — The hull trim angle in degrees. The angle of rotation of the hull coordinate system X-axis (or baseline) with respect to the earth coordinate system X-axis.

NPØS — The number of different vertical DELZ or horizontal DELX locations to be modeled for the previously given ICASE, IRHØ, and TRIMD. NPØS $\leq$ 100. See Card 14.

NVELS — The number of different velocity conditions to be considered for each NPØS. NVELS $\leq$ 10. See Card 10. Cards 6 through 14 define one operating condition. They must be repeated as a unit LAST times.

CARD 7 - Format (4I10)

ICALM — The option which dictates the type of impact being considered, calm water or wave. If ICALM = 1, it is a wave impact, and Card 8 will be read. If ICALM = 5, it is a calm water impact, and Card 8 must be omitted.

IWRITE — The option which controls the printout of the calculated impact pressure distributions. See the tabulation below.

IPG — The selected printout control option. All or individually selected transverse pressure distributions may be printed out. See the tabulation and Cards 12 and 13.

ICURVE — Pressure and load versus impact area relationships (PLA) may or may not be desired. See the tabulation.

IWRITE	IPG	ICURVE	Printing Operation
1	1	5	Total distribution and PLA relationships
1	1	1	Total distribution, no PLA relationships
1	5	5	Selected distributions and PLA relationships
1	5	1	Selected distributions, no PLA relationships
5	1	5	PLA relationships, no distributions
5	1	1	No printout

CARD 8 - Format (2F10.4)

WAVLEN The trochoidal wave length in inches.

AØVER2 The trochoidal wave amplitude in inches.

CARD 9 - Format (6F10.4)

YRWØ, YRWIN, YRWF The initial, the incremental, and the final values, respectively, for which transverse pressures are calculated on a normalized beam in the wet-chine region. For most cases, YRWØ = 0.0 and YRWF = 1.0. The value assigned to YRWIN depends on the desired mesh of the transverse distribution. For example, YRWIN could be set equal to 0.05.

YRDØ, YRDIN, YRDF Respectively same as above but with reference to the dry-chine transverse pressure distributions.

CARD 10 - Format (2F10.4)

VELØ The total horizontal hull velocity in inches per second.

VELVER The total vertical hull velocity in inches per second.

Card 10 must be repeated NVELS times. Cards 10 and 11 define one velocity condition within the operating condition unit. They must be successively repeated NVELS times.

CARD 11 - Format (2F10.4)

ØMEGA The rate of pitch of the hull about its center of gravity in radians per second. Clockwise motion is positive.

XCG The horizontal distance from the step to the hull center of gravity in inches.

Card 11 must be repeated NVELS times. See Card 10. XCG must be given in the same scale as the offset data on Card 4.

CARD 12 - Format (I10)

NPG The number of selected transverse pressure distributions to be printed out. NPG $\leq$ 15.

Card 12 is needed only if IWRITE = 1 and IPG = 5. See Card 7.

CARD 13 - Format (14I5)

LXKPG The selected station numbers for which transverse pressure distributions are to be printed out. The LXKPG values correspond to the N stations of Cards 2 and 4. As such, station locations must be identical to gage locations if this option is to be used.

Card 13 is needed only if IWRITE = 1 and IPG = 5. See Card 7.

CARD 14 - Format (2F10.4)

DELX — The X-coordinate of the origin of the hull coordinate system with respect to the wave profile crest. See Figure 13. If ICALM = 5 on Card 7, then DELX may be taken as 0.0 or any other arbitrary value.

DELZ — The Z-coordinate of the origin of the hull coordinate system with respect to mean water line. See Figure 13.

Card 14 must be repeated NPØS times.

According to the data setup and programming routines, only one hull per computer run may be analyzed during a hull-water impact. The option is available, however, to simulate several trim conditions, and types of impacts; calm water or waves. Additionally, the user may vary the horizontal and/or the vertical step locations at the given trim. In this way, the static analysis may be made quasi-static, provided that time histories of the trim, the velocities, and the step location are either known or assumed. The hull would then be incrementally stepped through the given wave profile or into the calm water impact.

The data set ZMNCHL must be fed in only if it has been decided that the incremental wedge trim angles are to be calculated by using the "mean-chine line." As a general rule, it may be said that for all hull cases, a mean-chine line should be constructed as described in the sample problem. It would then be used to calculate incremental wedge trim angles. In some cases, however, such a line would run approximately parallel to the keel. It may then be omitted and the keel used to calculate trim angles. The ZMNCHL option would be bypassed by letting IMCL be greater than 1.

Figure 12 is included to define the various hull geometry parameters necessary for input Cards 2 through 5. Data for the simulated conditions (input Cards 6 through 14) are explained graphically in Figure 13. Implicit type assignments are in effect for all integer and real variables.

EXPLANATION OF OUTPUT

The computer program presents output in several different forms. The extent or type of output is left as an option to the user. The forms in which this output can be presented are as follows.

1. A listing of input data, including the hull offsets. This output is not repeated since only one hull shape may be considered per run.

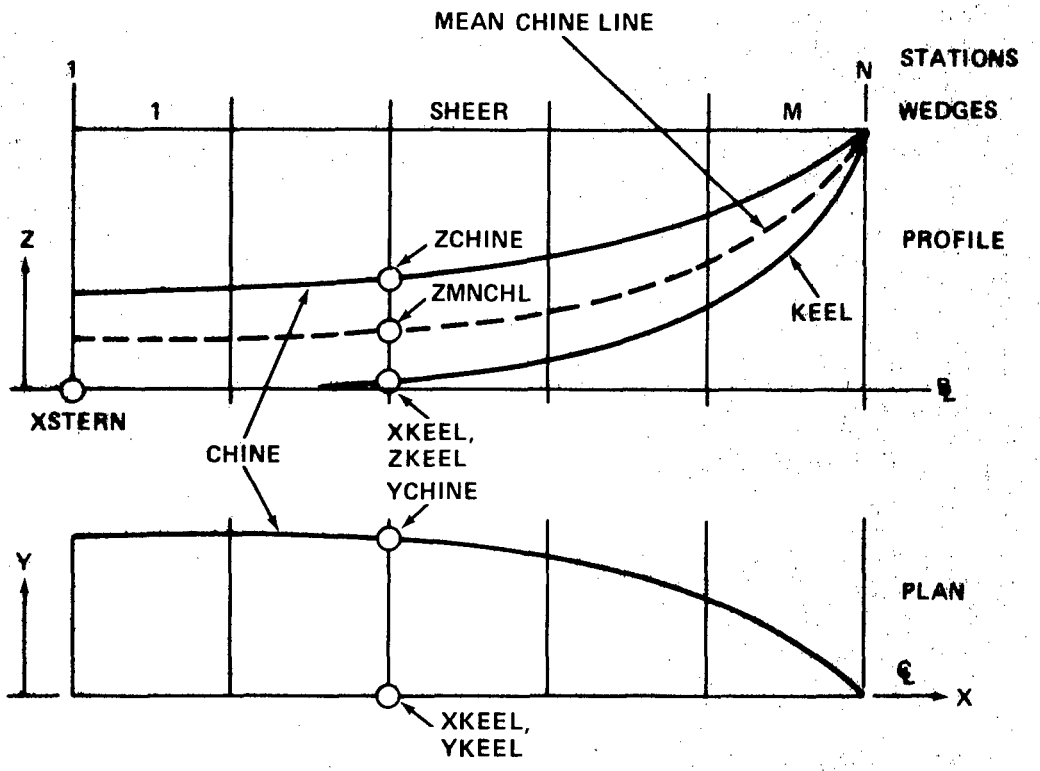

Figure 12 - Hull Geometry Parameters Required as Input Data

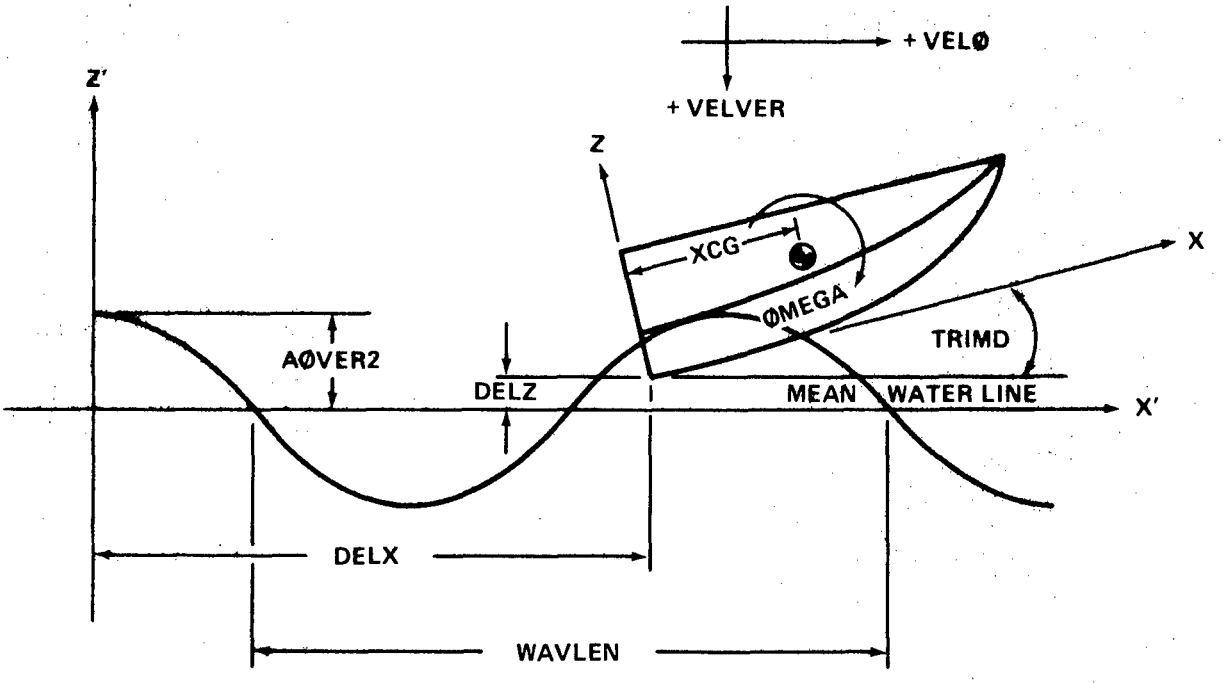

Figure 13 - Input Data for the Simulated Conditions

2. A description of the parameters chosen to describe the simulated condition, as well as the chosen output options. Additionally, the incremental wedges involved in the subsequent calculations are numerated, including the total wetted hull length.

3. A table which describes the characteristic parameters of each equivalent prismatic wedge corresponding to an incremental wedge. The information consists of the deadrise angle, the wedge trim angle, the corrected trim angle (hull trim accounted for), the wetted length in beams, and the immersion depth. In addition, the relative position of the incremental wedge on the total wetted length (X/X_m) is given.

4. A description of the assumed instantaneous velocities, including vertical, horizontal, and pitch rate components. The location of the center of gravity is also specified. This is a continuation of the input data listing.

5. A tabulation of the longitudinal distribution of horizontal and vertical forces, and the average true centerline pressure for each of the incremental wedges. Additionally, the total vertical and horizontal forces are given. Maximum pressure values P_m are based, in part, on the equivalent planing velocity $\dot{f}$ of Equation (2). The average value of $\dot{f}$ over the entire hull is included here as output.

6. A listing of the true centerline pressure for the boundary and midpoint stations of each wedge. Every third station of X/X_m is duplicated since it represents a boundary station on two adjacent wedges. The associated pressure will not necessarily be duplicated since the characteristic parameters of adjacent wedges may differ. Each station is also defined as either wet chine or dry chine. This output is controlled by the IWRITE option.

7. A full or partial listing of the transverse pressure distributions for the incremental wedges. Three stations are listed per wedge in terms of the mesh size Y/C chosen on Card 9 of the input. The Y/C values are given from Y/C = 0 to Y/C = 1.0, or to the point previous to a negative pressure value. This output is controlled by the IWRITE and IPG options.

8. A tabulation of the results of the isobaric contour integration routine. It includes information on the pressure ratio and load ratio versus the impact area ratio, the total normal impact force, the hull impact surface area, and the maximum detected pressure on the hull. This output

is controlled by the ICURVE option. A more detailed explanation of this output is given in Appendix D.

PROGRAM APPLICATION

Several experimental conditions[1] were simulated in order to demonstrate the capabilities of the impact analysis computer program, and the results obtained were compared to the experimental data and theoretical predictions presented by Chey.[1]

The simulated conditions involved two hull models, one of varying deadrise and one of constant deadrise, as shown in Figures 14 and 15, respectively. The simulations consisted of running the models through a regular trochoidal wave with a wavelength of 10 ft and a wave height of 9 in. double-amplitude. Three trim angles were considered--0, 5, and 10 deg bow up. The variable deadrise model had a horizontal velocity of 30 ft/sec whereas the constant deadrise model was run at 25 ft/sec. Vertical velocities and pitch rates were assumed to be zero for all conditions. Model keel heights above the mean waterline were defined in accordance with the conditions specified in Chey.[1]

The computer program was used to determine pressure distributions, peak impact pressures, pressure and load versus hull impact area relationships, and vertical and horizontal impact forces for all of the simulated conditions. The latter two forces are interpreted here to represent the impact-induced lift and drag forces, respectively. The comparisons discussed below, then, are made between the instantaneous force values as determined by the computer analysis and the experimentally determined average force amplitudes.

For the computer analysis, each of the specified operating conditions was simulated in a similar manner. This was accomplished first by specifying the initial conditions, or the hull step location relative to the mean waterline, the trim, and the horizontal velocity as defined in Chey.[1] The model was then made to incrementally "step" through the regular trochoidal wave by specifying several different horizontal positions of the hull step relative to the wave crest. As this was done, the initial conditions were held constant. The model was not allowed to surge, heave, or pitch in response to the wave-induced impact forces, and the velocity was not allowed to decay.

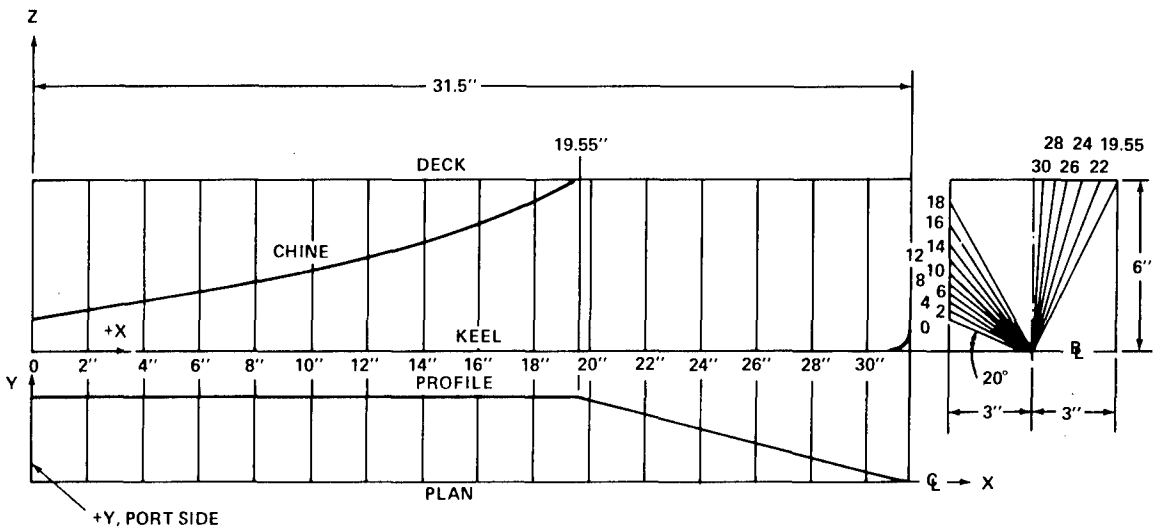

Figure 14 - Hull Lines of Model with Varying Deadrise

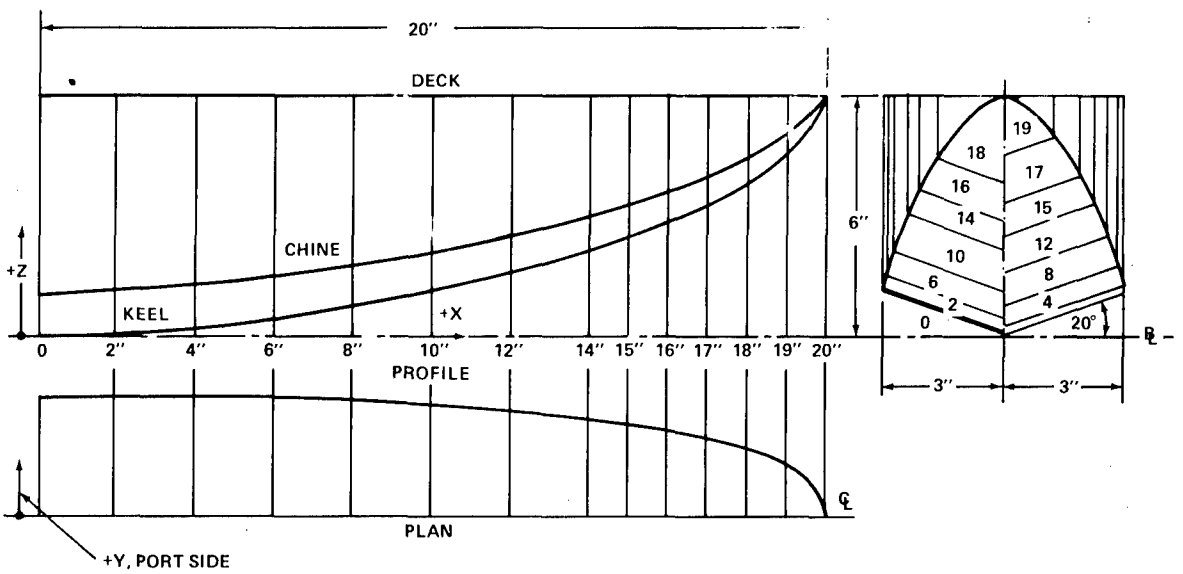

Figure 15 - Hull Lines of Model with Constant Deadrise

Figure 16 illustrates this procedure and the results obtained for several different horizontal step locations of the varying deadrise model at 10-deg trim in the 10-ft trochoidal wave. Each horizontal step position is defined by the ratio X_o/λ, an instantaneous relative location on the wave profile. Here X_o specifies the horizontal step location relative to the wave crest and λ is the wave length. This relationship is shown schematically below.

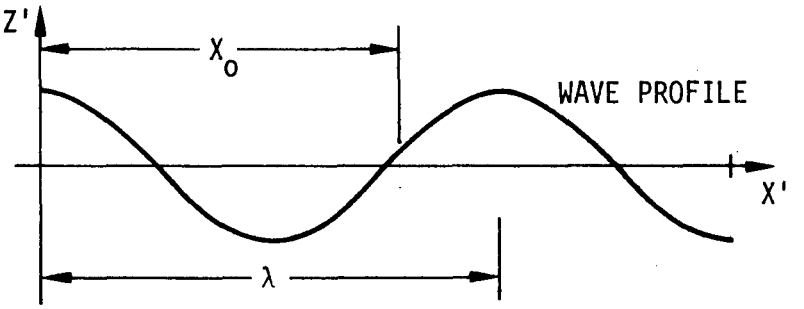

The computed impact-induced lift and drag forces acting on the two hull models are plotted as a function of X_o/λ in Figures 17 and 18 for all three trim conditions. The figures are intended to demonstrate the very significant rise in lift and drag caused by the hull-wave impact. Peaks in these curves appeared for X_o/λ values of 0.80 to 0.82.

Figures 19 and 20 demonstrate the correlation obtained between computer predictions and experimental data points for peak lift and drag forces for the varying-deadrise and constant-deadrise hulls, respectively. In addition, Figure 19 includes the Chey theoretical estimates based on strip theory and virtual mass.

It can be seen from Figures 19 and 20 that the impact-induced lift forces predicted by the computer analysis were consistently lower than the experimental data. On the other hand, the calculated drag did not display this consistency. Computed values were lower than experimental values for the varying-deadrise hull but higher for the constant-deadrise hull. However, Chey[1] states that his drag measurements are questionable because of instrumentation noise, and this could explain the discrepancy. Table 1 summarizes the calculated versus experimental correlation in terms of percent error and the ratio of experimental to predicted impact force magnitudes.

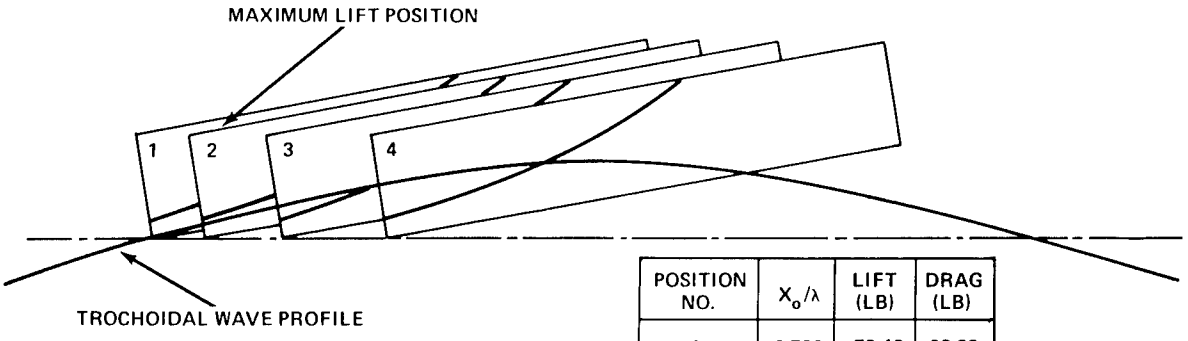

POSITION NO.	X_o/λ	LIFT (LB)	DRAG (LB)
1	0.790	79.46	23.22
2	0.803	111.28	31.27
3	0.843	64.88	19.85
4	0.895	57.54	17.40

Figure 16 - Lift and Drag at Various Wave Positions for Varying-Deadrise Model at 10-Degree Trim

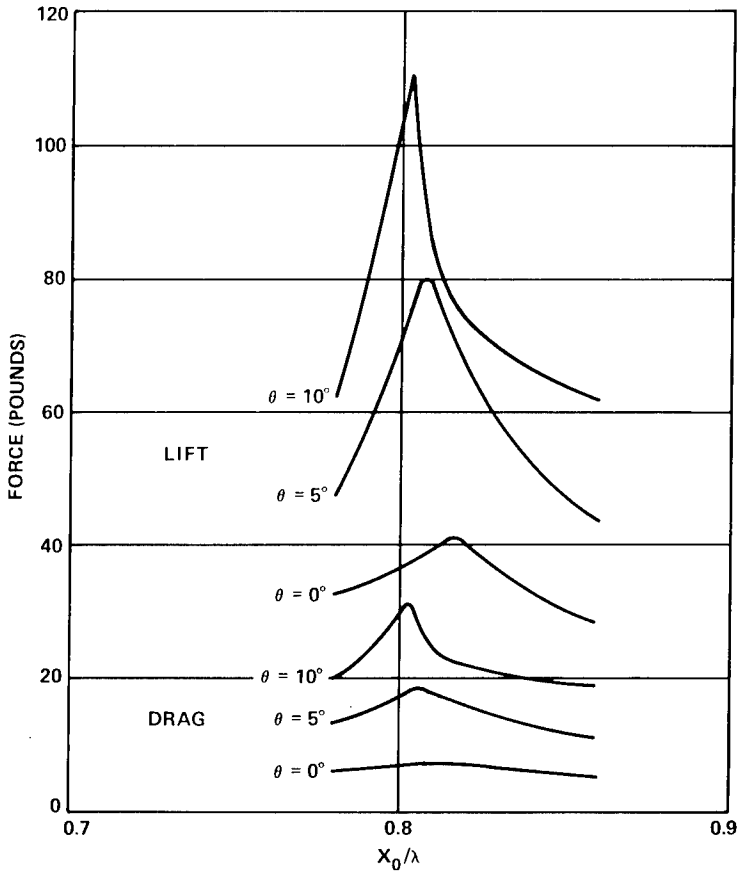

Figure 17 - Impact Lift and Drag Forces for the Varying-Deadrise Hull at Various Hull Step Locations and Trim Angles

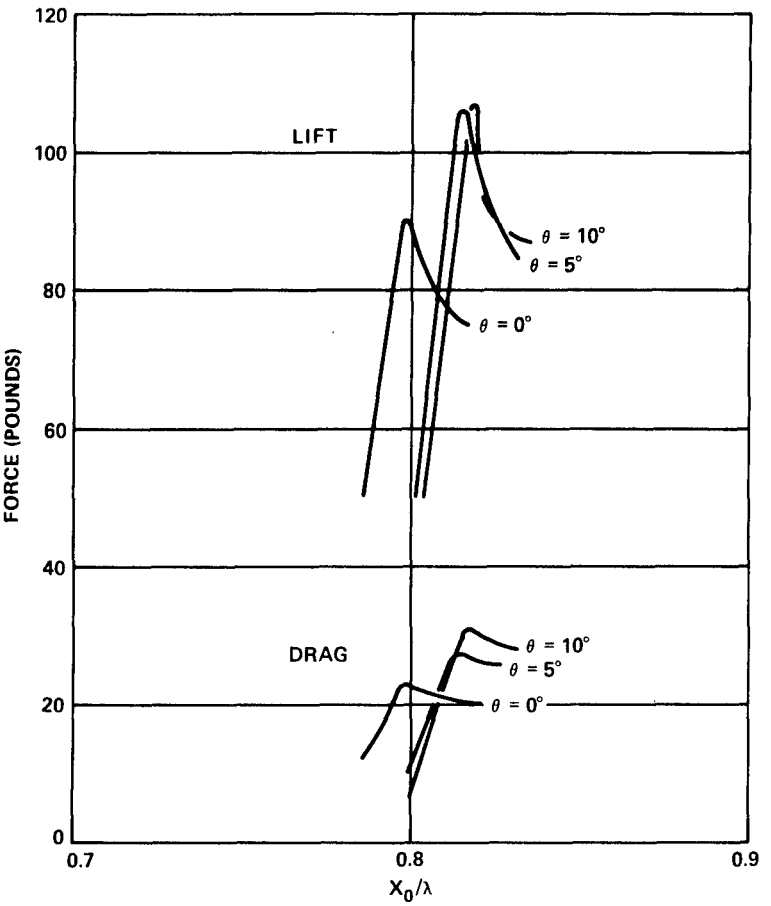

Figure 18 - Impact Lift and Drag Forces for the Constant-Deadrise Hull at Various Hull Step Locations and Trim Angles

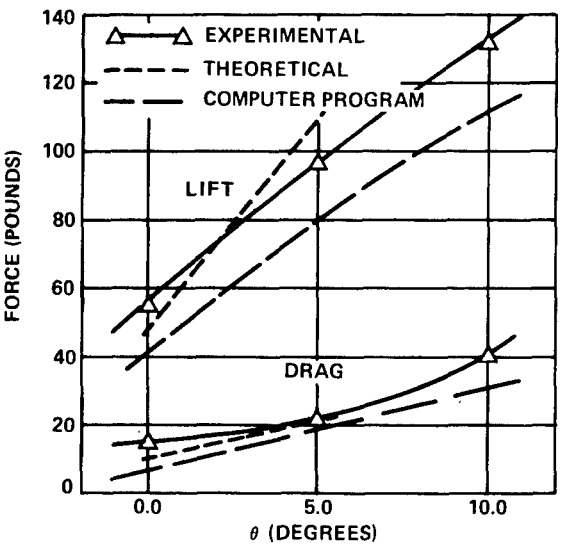

Figure 19 - Maximum Impact Lift and Drag Forces on the Varying-Deadrise Model at Various Trim Angles

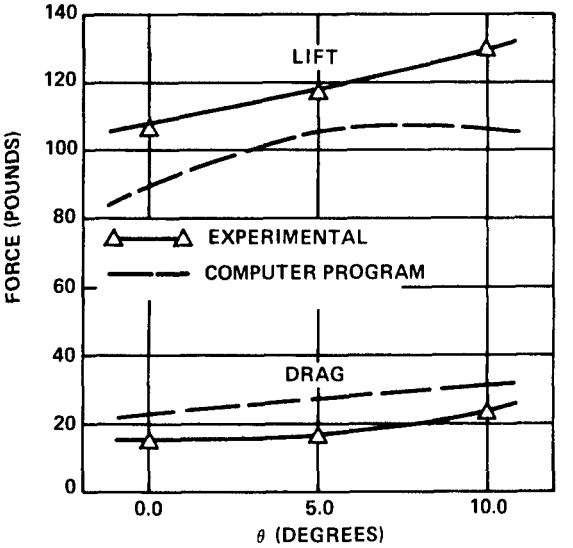

Figure 20 - Maximum Impact Lift and Drag Forces on the Constant-Deadrise Model at Various Trim Angles

TABLE 1 - SUMMARY OF COMPUTER PREDICTIONS VERSUS EXPERIMENTAL DATA FOR THE SIMULATED IMPACT CONDITIONS

Hull Model	Type Impact Force	Trim (deg)	Exp. (lb)	Comp. (lb)	Percent Error*	Exp./Comp.
Varying Deadrise	Lift	0	56	40.9	26.96	1.37
		5	97	80.2	17.32	1.21
		10	132	111.3	15.68	1.19
	Drag	0	15	7.2	52.00	2.08
		5	22.2	18.7	15.77	1.19
		10	40.5	31.3	22.72	1.29
Constant Deadrise	Lift	0	108	89.5	17.13	1.21
		5	118	105.7	10.42	1.12
		10	129.5	106.2	17.99	1.22
	Drag	0	15.8	22.7	-43.67	0.70
		5	17.0	27.3	-60.59	0.62
		10	24.0	31.1	-29.58	0.77

*[(EXP- COMP)/EXP] * 100

Figures 21 and 22 present a comparison of the computed and experimentally determined positions of peak impact lift. These figures, as well as Figures 19 and 20, are based on the plots shown in Figures 17 and 18.

One purpose of the computer analysis was to generate pressure and load versus hull impact area relationships for the six simulated operating conditions. One such relationship resulted from each of the incremental step locations as specified by the ratio X_o/λ. Figures 23 and 24 summarize the findings of the computer analysis. They include plots of the normal impact load L_o, the hull impact area A_o, the maximum detected impact pressure P_m, and the impact area to shell expansion area ratio A_o/A_T versus the instantaneous hull step location X_o/λ. Note that the magnitudes of the normal impact loads peaked at the same point as the impact lifts shown in Figures 17 and 18 and displayed the same tendency toward very sharply defined peaks.

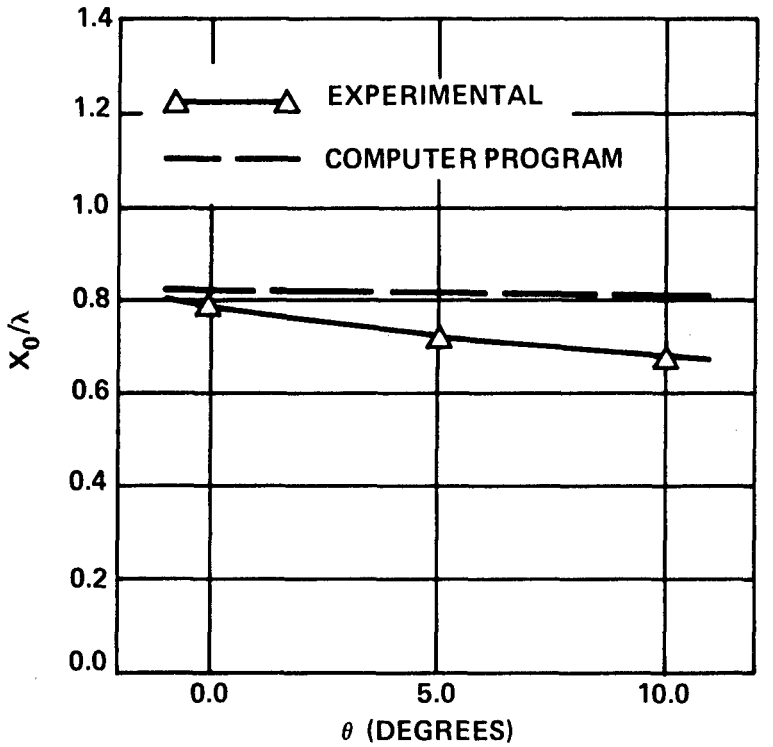

Figure 21 - Hull Step Location at Instant of Maximum Lift for the Varying-Deadrise Model at Various Trim Angles

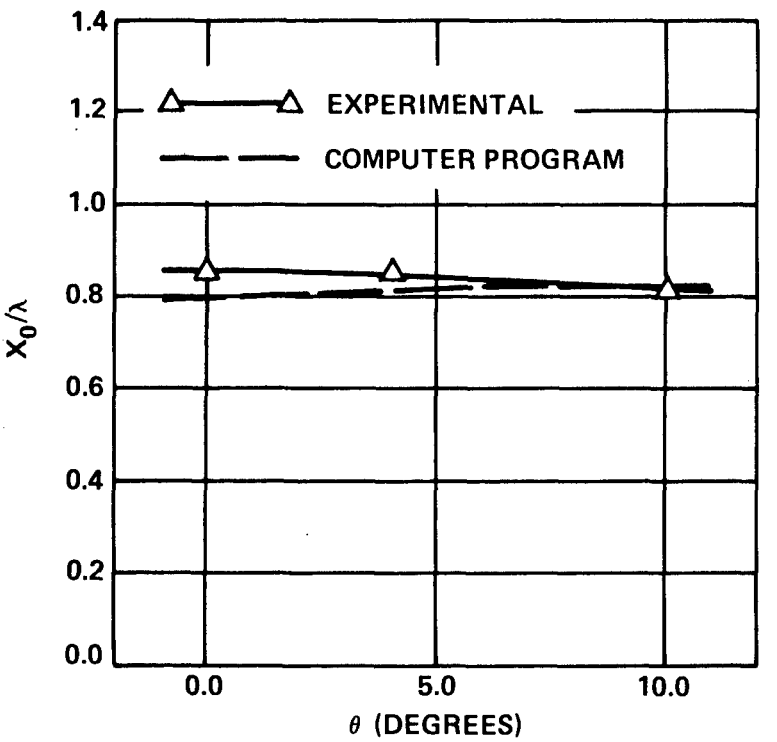

Figure 22 - Hull Step Location at Instant of Maximum Lift for the Constant-Deadrise Model at Various Trim Angles

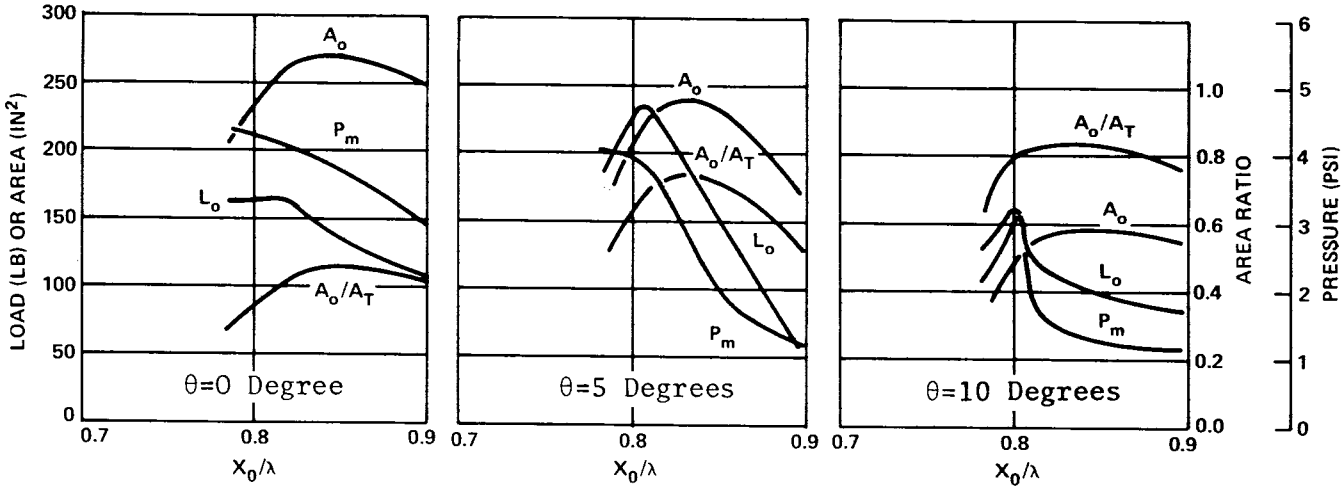

Figure 23 - Summary of Maximum Pressures, Normal Loads, Impact Areas, and Impact Area Ratios during the Hull-Wave Impact Simulations for the Varying-Deadrise Model at Various Trim Angles

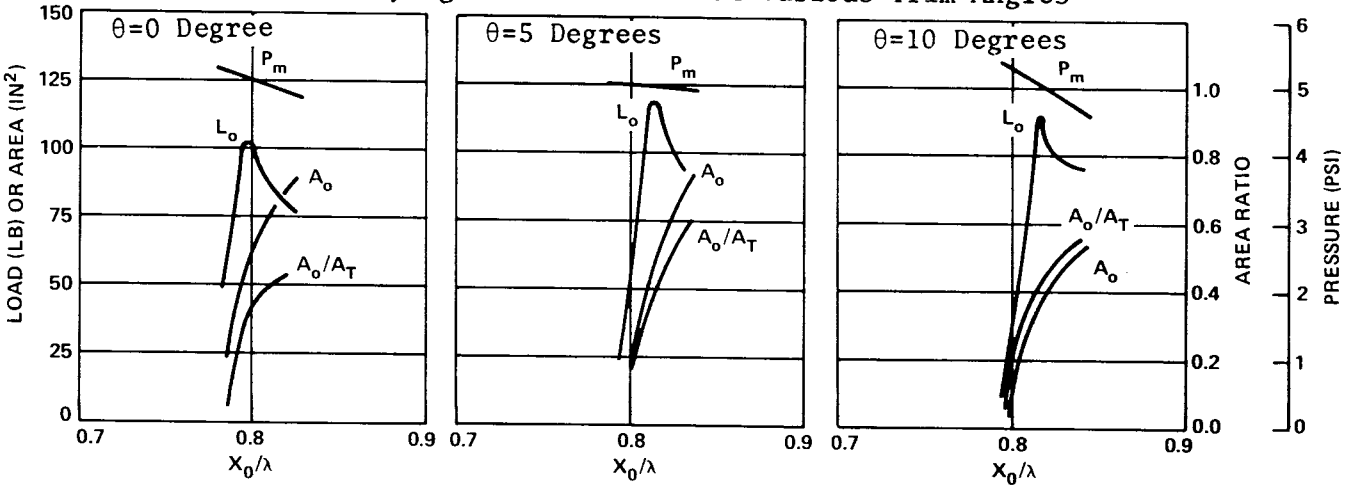

Figure 24 - Summary of Maximum Pressures, Normal Loads, Impact Areas, and Impact Area Ratios during the Hull-Wave Impact Simulations for the Constant-Deadrise Model at Various Trim Angles

Similar behavior may be attributed to the hull impact areas A_o shown in the figures. Their behavior was not characterized by sharply defined peaks. Further the instant of peak impact area did not coincide with the location of peak normal load and impact lift. This is attributable to the relationship between the magnitude and shape of the pressure distribution and the wetted surface area A_o at any instant in time.

Here we introduce the value A_T as the total possible load-bearing surface area, or the area defined by a shell expansion with the chine as the outer perimeter. The ratio of A_o/A_T is used to demonstrate the load concentration experienced during the hull-wave impacts. Figures 23 and 24 indicate that the peak impact lifts and normal forces did not coincide with the maximum ratio of A_o/A_T. The figures also show that A_o/A_T never exceeded 0.84, and that in most cases the values were far less. As can be seen by comparing A_o/A_T ratios, the varying-deadrise model made better use of the available load-bearing surface area, and thus more effectively reduced the impact load concentration than did the constant-deadrise model.

Figure 25 demonstrates the technique used to present the results of the computer simulations in a more meaningful way. This figure was generated by using the pressure-area relationships which resulted from the simulated hull-wave impact of the varying-deadrise model at a trim of 0 deg. Each model and trim angle combination was analyzed individually according to a similar scheme, as described below.

The pressure-area relationship values for the six instantaneous step locations X_o/λ were applied to a curve-fitting routine. The routine computed coefficients of the N^{th} degree polynomials by the least-squares method of curvilinear regression, minimizing the sum of the squared deviations from the average. It was then assumed that there was uniform scattering of the points about the regression curve and that the residuals $R = P - P_{CALC}$ were independent of each other and normally distributed about the regression curve. Since these conditions were assumed to be satisfied, statistical inferences could be made concerning the regression analysis. The routine was programmed to calculate the standard error of estimate σ which measures the average error of the regression curve in providing estimates of the dependent variable P from given values of the independent variable A/A_o. In this sense, it may be thought of as the standard

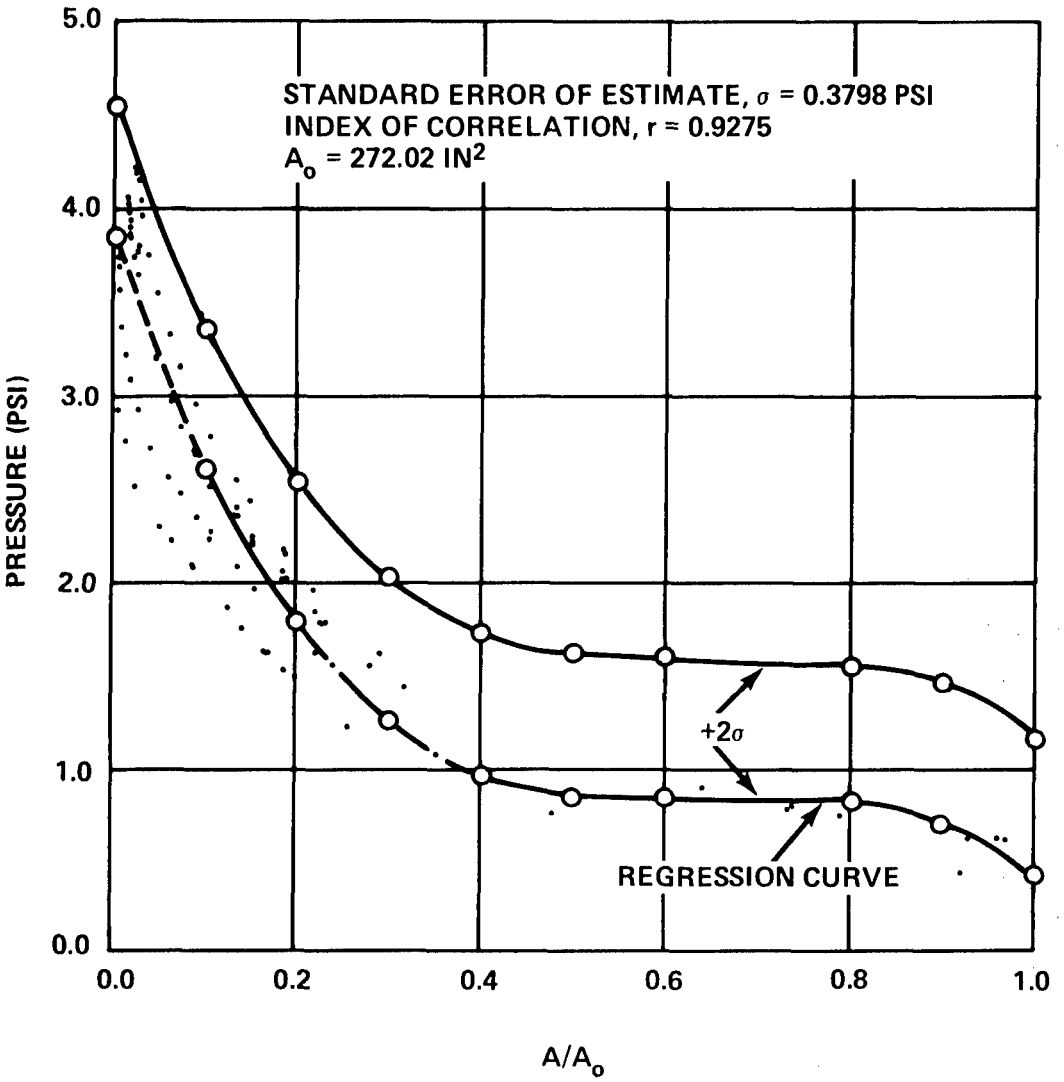

Figure 25 - Pressure-Area Points and Resulting Regression Curve from the Computer Simulation of the Varying-Deadrise Model at 0-Degree Trim

deviation of the residuals. Second, the routine calculated the index of correlation r. This provided a relative measurement of the relationship between two variables, or the proportion of the variation in the dependent variable which is accounted for by the independent variable. An index of r = +1.0 is considered perfect correlation for a regression curve sloping down and to the right.

Figure 25 shows the 120 points of pressure versus area used to generate the third-degree regression curve. In order to simplify the presentation the independent variable is given in a normalized form of A/A_o. A third-degree fit was utilized to minimize the occurrence of inflection points and yet still yield a fairly high index of correlation.

In addition to the regression curve, a similar curve is shown at a level which is +2.0 standard error of estimates greater. According to the assumption of normally distributed residuals about the regression curve, this curve signifies the upper bounds of the 95-percent confidence level for the determined regression curve. More exactly, the values defined by the regression curve $\pm 2.0\ \sigma$ include 95.45 percent of all the occurrences. The result is, then, a statistical method which may be used to forecast pressure-area relationships with some degree of certainty.

The pressure-area regression curve and the corresponding standard error of estimate were then used to develop the load-area relationship for the specified impact condition. The values were determined by calculating the product of the pressure and area at any point on the regression curve. Similarly, a family of load curves may be developed by increasing or decreasing the pressure values by an integer multiple of σ.

Figures 26 through 31 summarize the regression pressure-area curves and the corresponding load-area curves for each of the model and trim angle combinations. The standard error of estimate for each pressure-area curve may be used to produce the family of curves associated with the pressure and load curves shown here.

The analysis technique set forth here is not necessarily the optimum method of interpreting the computer predictions. Perhaps an envelope that encloses both the maximum and minimum values of the pressure-area and load-area values is more meaningful. However, the intent here was to present an analysis method with a certain degree of statistical reliability and

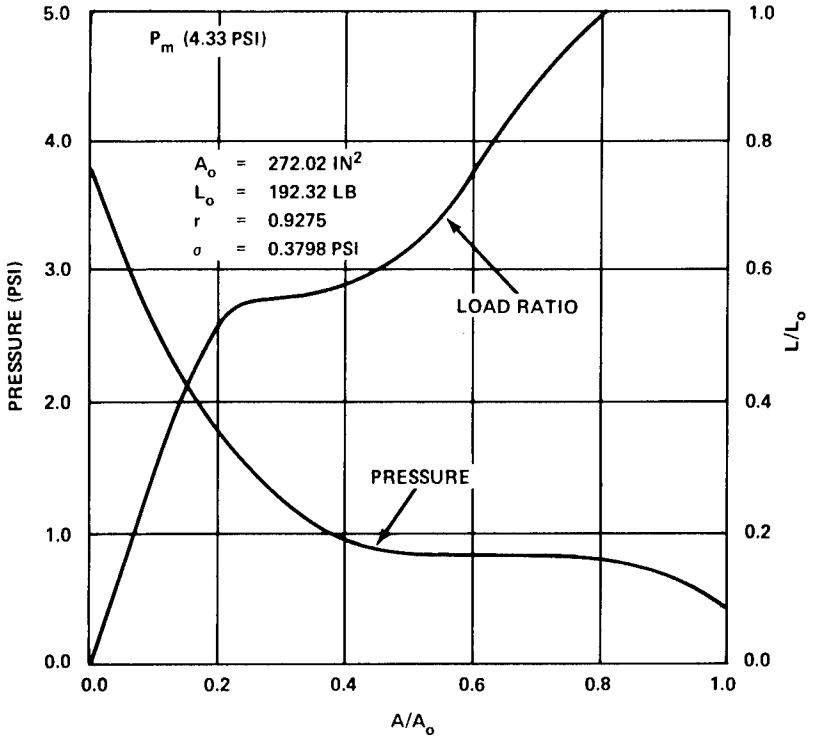

Figure 26 - Pressure and Load versus Impact Area Relationship for the Varying-Deadrise Model at 0-Degree Trim

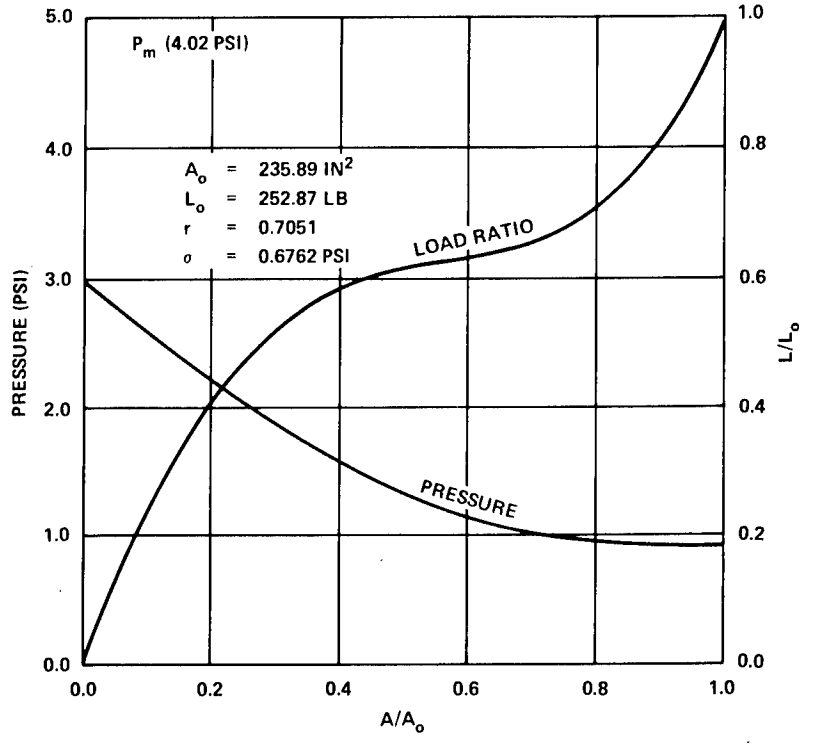

Figure 27 - Pressure and Load versus Impact Area Relationship for the Varying-Deadrise Model at 5-Degree Trim

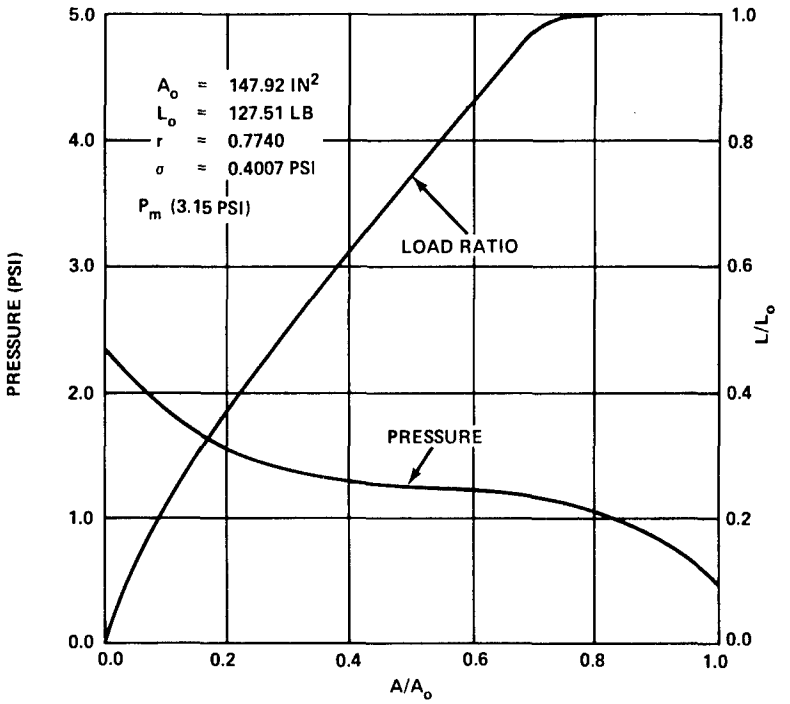

Figure 28 - Pressure and Load versus Impact Area Relationship for the Varying-Deadrise Model at 10-Degree Trim

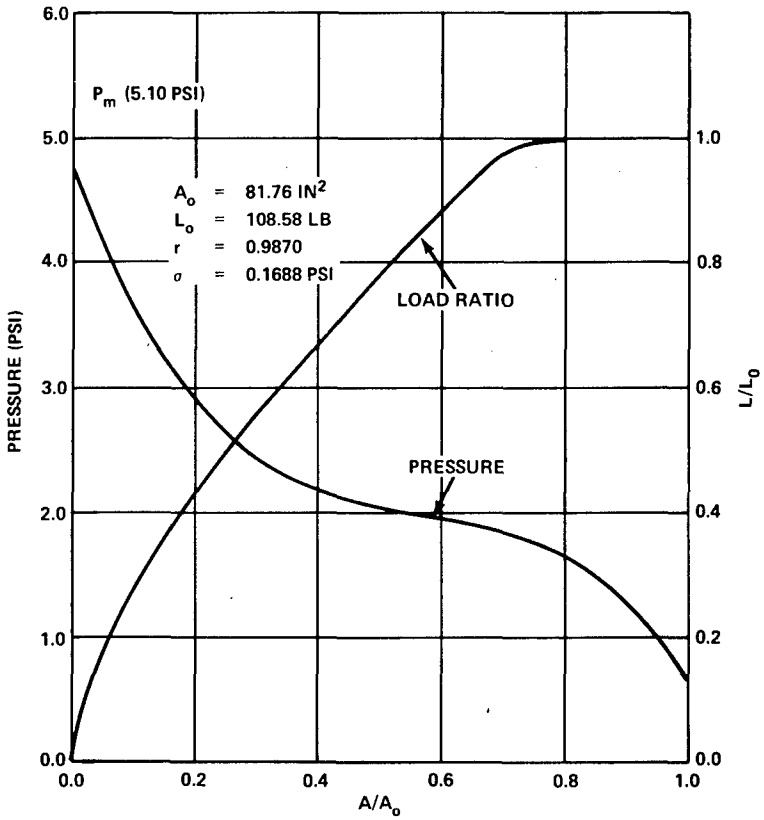

Figure 29 - Pressure and Load versus Impact Area Relationship for the Constant-Deadrise Model at 0-Degree Trim

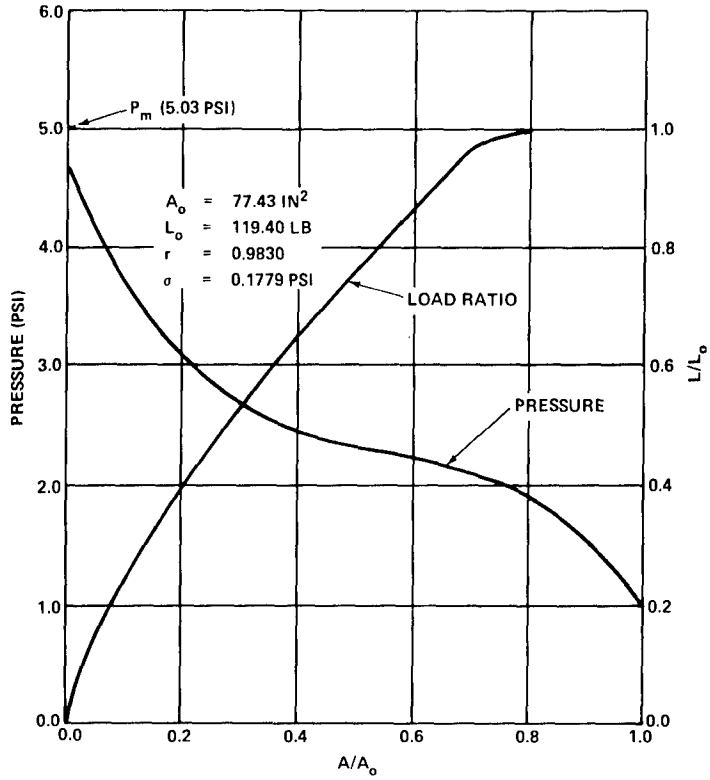

Figure 30 - Pressure and Load versus Impact Area Relationship for the Constant-Deadrise Model at 5-Degree Trim

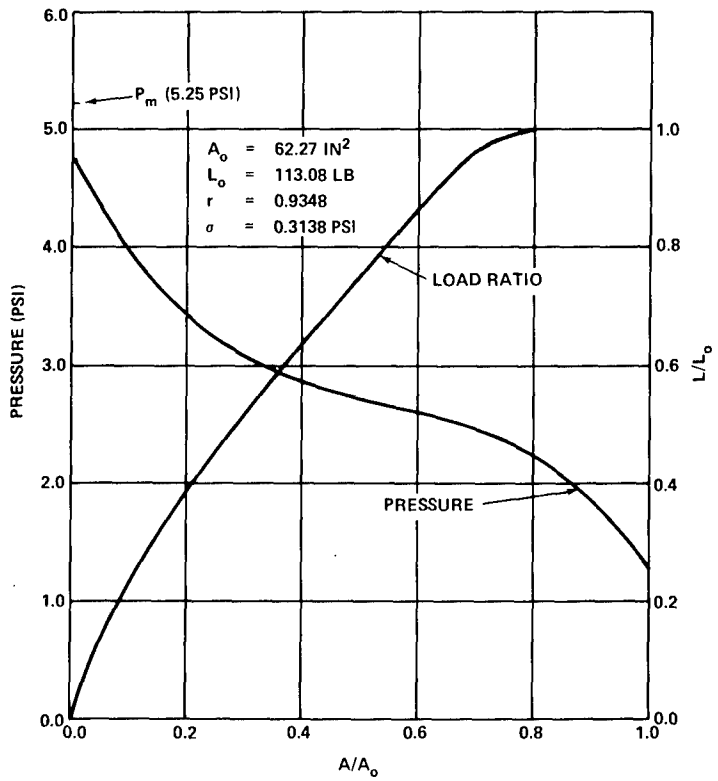

Figure 31 - Pressure and Load versus Impact Area Relationship for the Constant-Deadrise Model at 10-Degree Trim

predictability and one which allows the user to choose appropriate confidence levels for design purposes.

Admittedly, the preceding analysis technique has minor idiosyncracies. The most obvious one may be seen in Figure 25. The regression curve and corresponding standard error of estimate produce an excessively wide confidence band for values of A/A_o greater than 0.30. The width of this band depends of course on the scattering of the points and the resulting index of correlation. As can be seen from the plotted points, such a band is not representative of the computer predictions in this range. The regression analysis, however, does appropriately describe the pressure-area behavior in the region of primary design interest, $A/A_o < 0.10$, and thus may be justified.

For the most part, the regression pressure-area curve values produced a load-area curve which peaked out prior to $A/A_o = 1.0$. Only the varying-deadrise model at a trim of 5 deg escaped this oddity. By definition, the total normal load must be carried by the total wetted area, or $L/L_o = 1.0$, if and only if $A/A_o = 1.0$. It should be noted that the load-area relationships of Figures 26 and 28 through 31 have been plotted only out to $A/A_o = 0.8$ in direct contrast to the physical behavior of the impact phenomenon. As shown in Appendix D (Figure D.4), however, any one individual pressure-load-area relationship will satisfy the physical requirements.

This discussion of the pressure-load-area relationships has a twofold purpose: (1) to demonstrate the capabilities of the computer program and (2) to indicate how the results of the computer simulations may be interpreted and applied to the design of high-performance marine vehicles.

CONCLUDING REMARKS

The analysis technique presented in this report is operational. It represents a practical design tool which may be used to predict and describe the behavior of hull-bottom impact pressures on high-performance marine vehicles.

The results which the technique yielded for the simulated hull-wave impact vertical and horizontal forces are in reasonable agreement with experimental data. The concept of pressure-load-area relationships presented in this report is completely dependent on the maximum pressure and

the associated pressure distribution. The general trend of the relationships is considered to be accurate. However, further intensive experimental verification is necessary to ensure the accuracy of both the pressure magnitudes and the pressure-area relationships.

Extensive experimental data will soon be available for correlation with the analysis technique predictions. These data include both model and full-scale tests and will provide a basis for comparing both pressure magnitudes and pressure-area relationships. It is expected that the agreement between experimental and analytical results will be more convincingly demonstrated when these recent, carefully controlled trial data become available.

In fact, a limited number of simulations have already been conducted by using these data. Preliminary findings indicate that excellent correlation can be expected between predictions and experimental data. The reliability and accuracy of the method and the conclusions of these studies will be the subject of future reports.

FUTURE DEVELOPMENTS

The ever-expanding future of high performance, dynamically supported marine vehicles indicates the need to further develop the understanding of environmental loadings, such as hull-wave impacts. The analysis method presented here represents part of a continuing effort to produce a comprehensive design tool whose end product is rational design criteria. It is not, however, the ultimate tool but rather a foundation on which to build. Listed below are some areas which the authors feel constitute valid tasks for future research and development.

1. Utilize recent additional experimental data to update and improve the theoretical methods of predicting maximum impact pressure on three-dimensional immersing wedges.

2. Conduct a series of controlled experiments to determine whether wave particle orbital velocity and/or wave propagation velocity should be included in the calculation of impact pressures.

3. Account for the hull rigid body dynamic response to a simulated wave encounter, for example, by using a six-degree-of-freedom motion simulation program.

4. Couple the impact analysis technique with an analysis method which will determine the longitudinal force, shear, and moment distributions that result from the simulated hull-wave impact.

5. Investigate further the use and application of pressure-load-area relationships and their ability to provide a basis for rational design criteria of hull scantlings.

6. Update the user qualities of the method by including active graphics for input, contour plotting of constant pressure lines, and graphic output of pressure-load-area relationships.

All of these suggestions are important to facilitate more widespread designer usage of the analysis method provided in this report.

ACKNOWLEDGMENT

The authors are greatly indebted to Mr. Harry P. Gray. His initial work in developing a computerized method for predicting pressure distributions on V-shaped prismatic wedges laid the foundation for the analysis technique reported herein.

APPENDIX A

TROCHOIDAL WAVE APPROXIMATION

Maximum hull-wave impact pressures are, in part, a function of the wave particle orbital velocity. For gravity waves, the orbital velocity is, in turn, a function of wave length, wave height, depth, and local acceleration due to gravity. Some investigators prefer to include the wave celerity in maximum pressure calculations. However the authors feel that at the present time, data are insufficient to warrant its use. It is, therefore, not included in the present method of calculating maximum pressures.

Historically, the trochoidal wave has been used to describe the profile for finite amplitude waves. It differs from an harmonic (i.e., sinusoidal) deep-water wave at the crest, where it is sharper, and at the trough, where it is flatter, as shown in Figure A.1. However, for wave heights up to $\lambda/20$, it more closely approximates the simple wave form in a wave tank and as observed on the open sea and thus has merit for incremental wedge modeling.

Equivalent prismatic wedges are a direct function of the incremental wedge immersion depth ℓ. Since the size of the equivalent prismatic wedge dictates the magnitude and shape of the final pressure distribution, accurate determination of the immersion depth is essential. For this reason, the trochoidal wave profile is utilized in the computer analysis.

Although the profiles are different, the basic relationships for an harmonic wave are applicable to a trochoidal wave. For the following discussion of a trochoidal wave profile, then, the velocity and period to length relationships used are those given by Korvin-Kroukovsky[8] and shown in Figure A.2.

---

[8]Korvin-Kroukovsky, B. V., "Theory of Seakeeping," Society of Naval Architects and Marine Engineers, New York, N. Y. (1961).

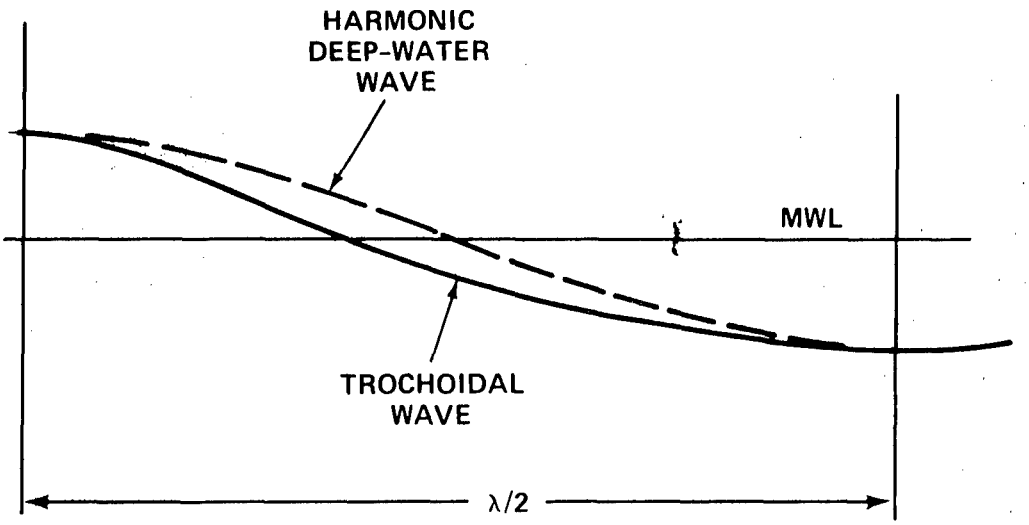

Figure A.1 - Surface Profiles of Harmonic and Trochoidal Waves

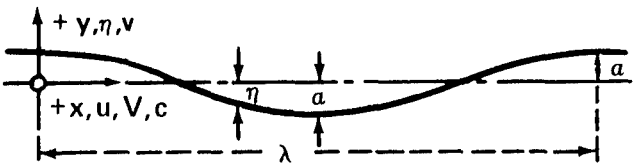

Figure A.2 - Properties of Trochoidal Waves

(From Korvin-Kroukovsky[8])

The parametric expressions for a trochoidal wave are

$$x = R\theta + r \sin \theta \tag{A.1}$$

$$y = R + r \cos \theta \tag{A.2}$$

where R, r, and θ are defined in Figure A.3. The intrinsic nature of these expressions requires an iterative technique to calculate y, the wave height, in terms of x, any position along the wave profile.

In an effort to minimize computer time, the trochoidal wave profile is represented by a cosine series approximation. The wave profile can be given with sufficient accuracy by the expression developed by Vossers and presented in a report by Muckle.[9] The wave height y in terms of longitudinal wave position x is given by

$$y = r \cos \frac{2\pi x}{\lambda} - \frac{\pi r^2}{\lambda} \left(1 - \cos \frac{4\pi x}{\lambda}\right) \tag{A.3}$$

where r is the wave amplitude, as in Figure A.2, and λ is the wave length.

The wave particle orbital velocity horizontal and vertical components at any point (x, y) on the wave profile are then given by

$$W_h = V \sin kx \tag{A.4}$$

$$W_v = V \cos kx \tag{A.5}$$

$$V = krC_H e^{ky} \tag{A.6}$$

where $k = \frac{2\pi}{\lambda}$ is the wave number,

$C_H = \left(\frac{g\lambda}{2\pi}\right)^{1/2}$ is the wave celerity,

---

[9]Muckle, W., "A Note on the Buoyancy of a Ship Amongst Waves," Trans. Royal Institute of Naval Architects, pp. 549-557 (1965).

r is the wave amplitude,

λ is the wave length, and

g is the gravitational acceleration.

This process is repeated for each incremental wedge transverse pressure distribution and is based on its relative longitudinal position on the surface of the wave profile.

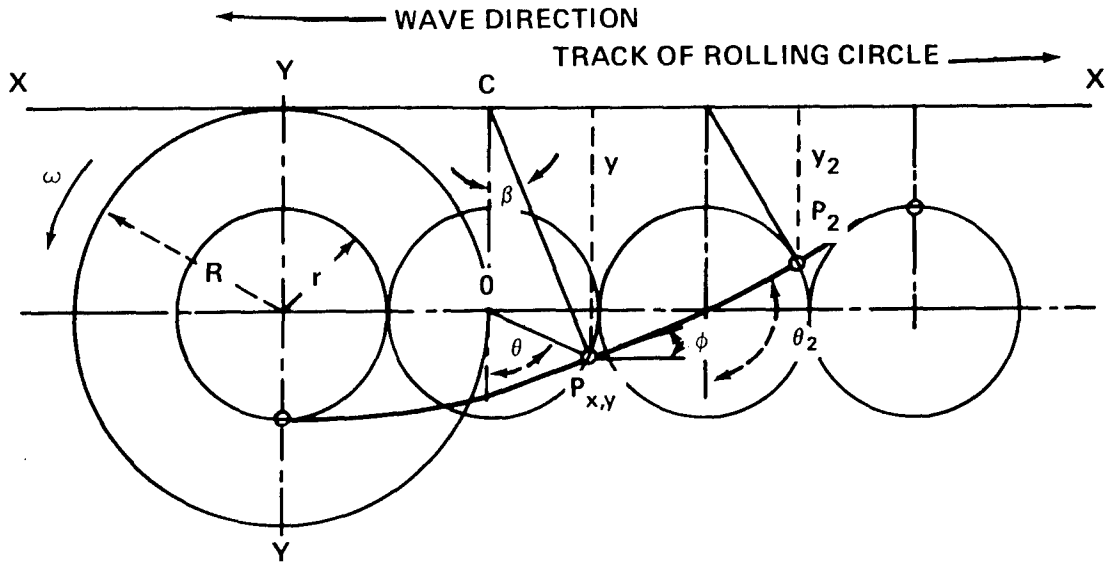

Figure A.3 - Geometry of a Trochoid

(From Korvin-Kroukovsky[8])

APPENDIX B

CALCULATION OF THE MAXIMUM IMPACT PRESSURE

According to Smiley,[5] the maximum impact or planning pressure P_m may be found by

$$P_m = \frac{1}{2} \rho \dot{f}^2 \tag{B.1}$$

where

$$\dot{f} = \dot{X}' + \dot{Z}' \cot \tau = \frac{\dot{Z}}{\sin \tau} \tag{B.2}$$

The inherent deficiencies of Equation (B.1) have been previously discussed for low trim angles τ. As $\tau \to 0.0$ deg, the value of P_m can be seen to approach infinity since $\dot{f} \to \infty$. Such behavior raises serious questions regarding the validity of Equations (B.1) and (B.2).

In order to remedy this situation, the empirical equations derived by Chuang and Milne[7] are included in the calculation of P_m. Their investigation concerned impacts for two-dimensional wedges and three-dimensional cones with *deadrise* angles of 15 deg and less. However, interest here centers about the cases for which the *trim* angle approaches zero. The assumption was made, then, that the behavioral characteristics ascribed to variations in the deadrise angle are quantitatively the same as those for variations in the trim angle. Such a widespread assumption requires justification.

Impact may broadly be divided into two basic types, purely vertical and a combination of vertical and horizontal components. First consider purely vertical impact. For this type of impact, $\dot{X}' = 0.0$, $\dot{Z}' > 0.0$ and $\dot{f}$ becomes

$$\dot{f} = \dot{Z}' \cot \tau \tag{B.3}$$

As τ approaches 0.0 deg, $\dot{f}$ approaches infinity, as does P_m. In the normalized form of Equation (6), P_m may be expressed as

$$P' = P_m / \frac{1}{2} \rho V^2 \frac{1}{144}$$

$$= \cot^2 \tau \qquad \text{(B.4)}$$

where V is replaced by $\dot{f}$.

This behavior of P' is compared to the behavior of P_m for the Chuang-Milne two-dimensional wedges. In normalized form

$$P' = \pi \cot \xi \qquad \text{(B.5)}$$

where ξ is defined by Equations (7) for $\beta > 1.0$ deg. For $\beta = 0.0$ deg and $\beta = 1.0$ deg, respectively, P' is given by

$$P' = 127.5$$

and (B.6)

$$P' = 148.9$$

Here, ξ is defined as the effective impact angle and is a function of both the deadrise and trim angles.

As shown by Equation (15) of Gray et al.,[4] the final value of P_m is a function of the deadrise angle. However, Equation (B.3) itself is not, and the correction for P_m or P' based on the deadrise angle is cosine β. For demonstration purposes, however, Figure B.1 compares Equation (B.4) to Equations (B.5) and (B.6). The inclusion of the cosine β term, Equation (B.4), merely generates a family of curves below that shown in Figure B.1.

Figure B.1 indicates the very basic differences between the two equations. For the range of 0 to 17 deg, $P' = \cot^2 \tau$ generates values greater than $P' = \pi \cot \xi$. Beyond 17 deg, the opposite is true. However, the curve for $P' = \pi \cot \xi$ indicates finite values for P' at low trim angles, a fact which bears out the idea of a finite spray root velocity.

Since the curve for $P' = \pi \cot \xi$ is based on recently published experimental data, it is used to calculate P_m for entirely vertical impacts. Again, ξ is the effective deadrise angle as derived in Chuang and Milne[7] and it is a function of the trim τ, the deadrise angle β, the horizontal

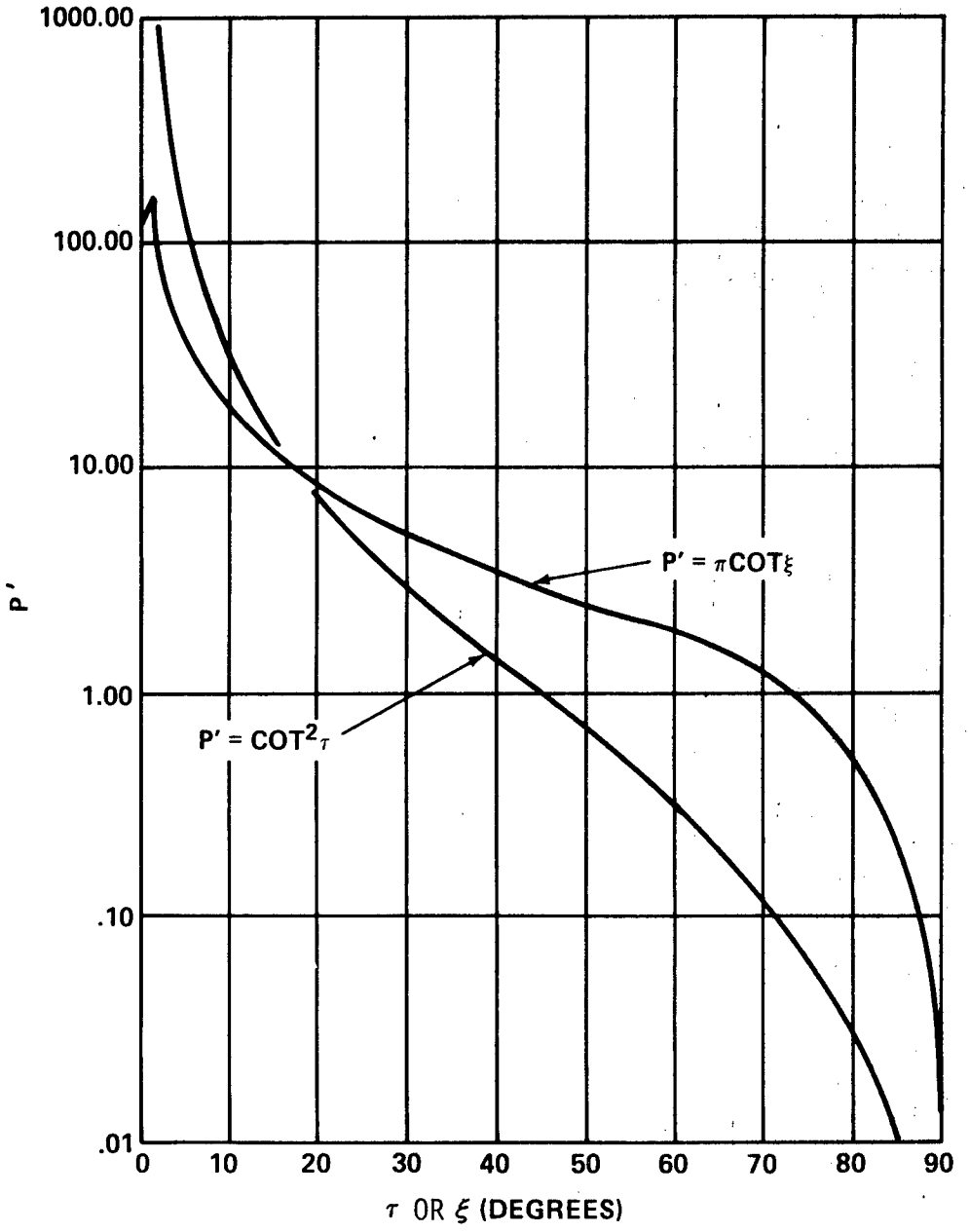

Figure B.1 - Normalized Curves for P' during a Vertical Impact Condition

effective deadrise angle β_{EH}, and the vertical effective deadrise angle β_{EV}. A schematic derivation of β_{EH} and β_{EV} is given by Chuang.[6]

A similar comparison may be made for impacts which are a combination of vertical and horizontal velocities. Here, $\dot{X}' > 0.0$, $\dot{Z}' > 0.0$, and $\dot{f}$ becomes:

$$\dot{f} = \dot{X}' + \dot{Z}' \cot \tau = \frac{\dot{Z}}{\sin \tau}$$

As τ approaches zero, $\dot{f}$ and P_m again approach infinity. In the normalized form of Equation (6), P_m becomes

$$P' = \frac{P_m}{\frac{1}{2} \rho V^2 \frac{1}{144}}$$

$$P' = \frac{1}{\sin^2 \tau} = \csc^2 \tau \qquad \text{(B.7)}$$

where this time V is replaced by $\dot{Z}$. The behavior of P' is given in Figure B.2.

At present, unfortunately, no recent experimental data are available which deal with the type of impact where both $\dot{X}'$ and $\dot{Z}' > 0.0$. Figure B.2 demonstrates the behavior of these values for $\tau \leq 15$ deg as well as the final corrected curve used for an impact where $\dot{X}'$ and $\dot{Z}' > 0.0$.

The assumptions made for determining P_m are subject to close scrutiny. However, comparisons with available experimental data indicate that they are not unjustifiable. Moreover, when new data become available, the subroutine format used in the computer program allows for their incorporation. The dilemma of restricting the behavior of Equation (B.7) to finite values as τ approaches zero must then be based on an assumed correction.

Chuang and Milne present empirical relationships for P_m based on experimental data for impacting three-dimensional cones with deadrise angles of 15 deg and less.[7] These relationships are used to restrict the behavior of P_m below $\tau = 15$ deg according to the assumption that β and τ are identical for the cones and $V = \dot{f}$ in P_m. Table B.1 presents these empirical equations and their corresponding P' values.

TABLE B.1 - VARIATIONS IN THE MAXIMUM PRESSURE AND NORMALIZED PRESSURE VALUES AS A FUNCTION OF THE DEADRISE ANGLE FOR THREE-DIMENSIONAL CONES

(Values in the middle column are from Chuang and Milne[7])

β deg	P_m psi	P'
0	$0.320\ \rho\ V^2$	92.2
1	$1.160\ \rho\ V^2$	334.1
3	$0.562\ \rho\ V^2$	161.9
6	$0.273\ \rho\ V^2$	78.6
10	$0.134\ \rho\ V^2$	38.6
15	$0.072\ \rho\ V^2$	20.7

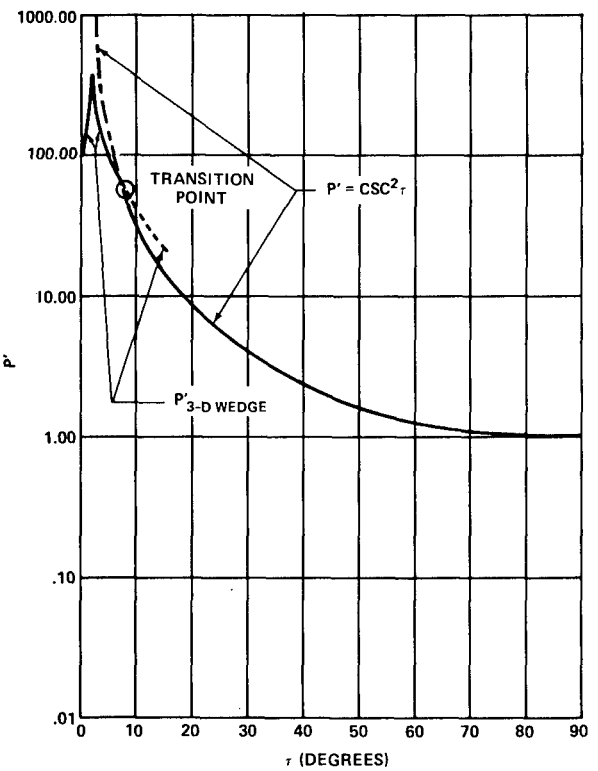

Figure B.2 - Normalized Curves for P' during an Impact with Horizontal and Vertical Velocity Components

APPENDIX C

EXAMPLE OF ISOBARIC INTEGRATION

Contour or isobaric integration describes the relationships which exist between the pressure, load, and surface area during a hull-water impact. This is accomplished by performing repetitive operations using isobaric contours and the analysis technique described previously. The simple example included here is meant to demonstrate the technique and its application to panel design.

Consider a square, flat-bottom plate subject to a hypothetical external pressure load. The pressure is assumed to be pyramidally distributed, as shown in Figure C.1a, and to range from zero to a P_m of 10 psi. The total load-bearing surface area of the plate A_T is set equal to the impact area A_o of 100 in.^{2}. Isobaric contours P_i are taken every 2 psi for a total of five contours.

The repetitive process is initiated by choosing P_5 = 8 psi and defining A_5 according to Equation (8) as the area for which $P_5 < P \leq P_6$ or $8 < P \leq 10$ psi. The area A_5, which is shown on Figure C.1b, is found to be 4 in.^{2}. By using Equations (9) and (10) of this report (page 16) the load L_5 is given as

$$L_5 = \overline{P}_5 A_5$$

$$= 9 \times 4$$

$$= 36 \text{ lb}$$

For this isobar, the area A_5' defined by Equation (12) is

$$A_5' = \sum_{k=5}^{5} A_k$$

$$= A_5$$

$$= 4 \text{ in.}^2$$

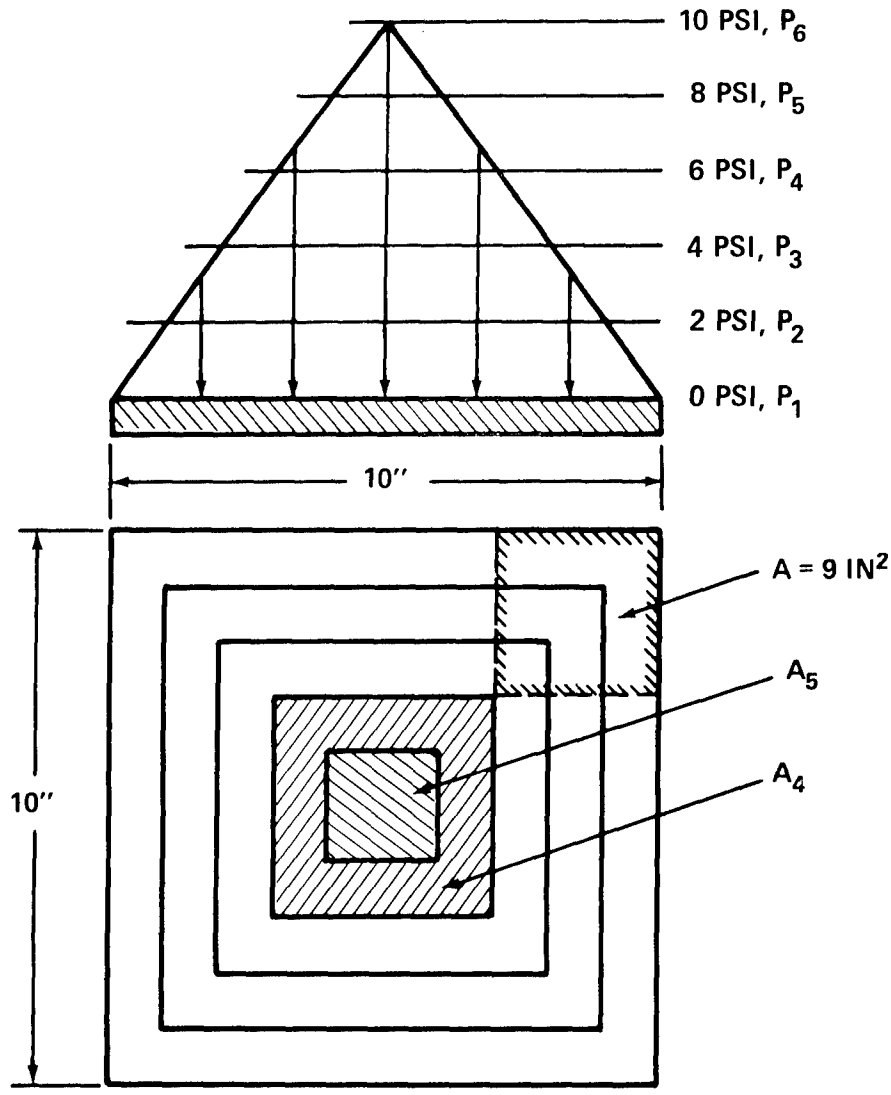

Figure C.1 - Example of Isobaric Integration on a Square Plate Subject to a Hypothetical External Pressure Load

and according to Equation (13) of this report the load L_5' is

$$L_5' = \sum_{k=5}^{5} L_k$$

$$= L_5$$

$$= 36 \text{ lb}$$

The true average pressure acting on A_5' is then found by using Equation (14) of this report:

$$P_5' = \frac{L_5'}{A_5'}$$

$$= \frac{36}{4}$$

$$= 9 \text{ psi}$$

Next, choose $P_i = P_4 = 6$ psi and calculate A_4 as the area for which $6 < P \leq 8$ psi. Figure C.1b depicts the area representative of this pressure region, which is found to be $A_4 = 12$ in.^{2}. Then, the load L_4 is

$$L_4 = \overline{P}_4 A_4$$

$$= 84 \text{ lb}$$

Similarly, A_4', L_4', and P_4' are found to be

$$A_4' = \sum_{k=4}^{5} A_k \qquad L_4' = \sum_{k=4}^{5} L_k \qquad P_4' = \frac{L_4'}{A_4'}$$

$$= 12 + 4 \qquad = 84 + 36 \qquad = \frac{120}{16}$$

$$= 16 \text{ in.}^2 \qquad = 120 \text{ lb} \qquad = 7.5 \text{ psi}$$

Up to this point, the pressure and load characteristics have been defined for two distinct areas of the plate. The area A_5' is unique in that it represents the area of highest pressure, and, therefore, of highest load concentration. In this respect, its behavior is independent of the other incremental areas.

In contrast, A_4' is not a unique area since it contains A_5'. The load and average pressure of A_4' are, then, a function of two distinct incremental areas. This has the effect of increasing the load concentration of A_4'. Thus, although $\overline{P}_4$ indicates only 7.0 psi, P_4' has a value of 7.5 psi.

The remaining incremental areas which are defined by pressure contours are also affected by this additive characteristic of pressure distributions. Therefore, the development of pressure and load relationships for the entire plate requires that the process be repeated for the remaining contours. The results of such an operation are summarized in Table C.1 where area, pressure, and load are normalized to their maximum respective values. A graphical presentation of the results is given in Figure C.2.

The value of area-pressure-load relationships lies in their usefulness to the designer. In this example, if the plate is assumed to represent a hull bottom, the curves in Figure C.2 may be used to provide design information for a typical panel. The process involves (1) defining the ratio of the panel area to the impact area, A/A_o and (2) entering the curves of Figure C.2 to find the corresponding pressure ratio P/P_m and the load ratio L/L_o. Then, with P_m and L_o known, the design pressure and load for the panel may be calculated.

If a panel size of 9 $in.^2$ is assumed, the area ratio becomes $A/A_o = 9/100 = 0.09$. By using the curves of Figure C.2, it is found that $P/P_m = 0.82$ and $L/L_o = 0.22$. Table C.1 is then used to define P_m and L_o as 10 psi and 340 lb, respectively. Finally, the design information indicates that the selected panel must be capable of withstanding 8.3 psi and carrying a load of 71.4 lb.

This, of course, is representative of the selected pressure distribution. As noted previously, each impact is a unique event, giving an equally unique relationship for the pressure and load versus the impact area. The limited number of impact examples and data provided in this report

TABLE C. 1 - SUMMATION OF RESULTS FROM THE EXAMPLE OF ISOBARIC INTEGRATION

	$\overline{P}_i$	A_i	$\overline{P}_i A_i$ (L_i)	ΣA_i (A_i')	ΣL_i (L_i')	P_i'	A/A_o	P/P_m	L/L_o
i	Average Pressure $\frac{P_i + P_{i+1}}{2}$ psi	Partial Impact Area, Where $P_i < P \leq P_{i+1}$ $in.^2$	Partial Load Carried by A_i lb	Total Impact Area, Where $P \geq P_i$ $in.^2$	Total Load Carried by A_i' lb	True Average Pressure for Area A_i'	Hull Impact Surface Area Ratio	Impact Pressure Ratio	Normal Load Ratio
1	1	36	36	100	340	3.40	1.00	0.340	1.000
2	3	28	84	64	304	4.75	0.64	0.475	0.890
3	5	20	100	36	220	6.10	0.36	0.610	0.650
4	7	12	84	16	120	7.50	0.16	0.750	0.350
5	9	4	36	4	36	9.00	0.04	0.900	0.106

indicate, however, that curve shape generalizations may be in order. This aspect of the relationships is discussed further in the sample problem.

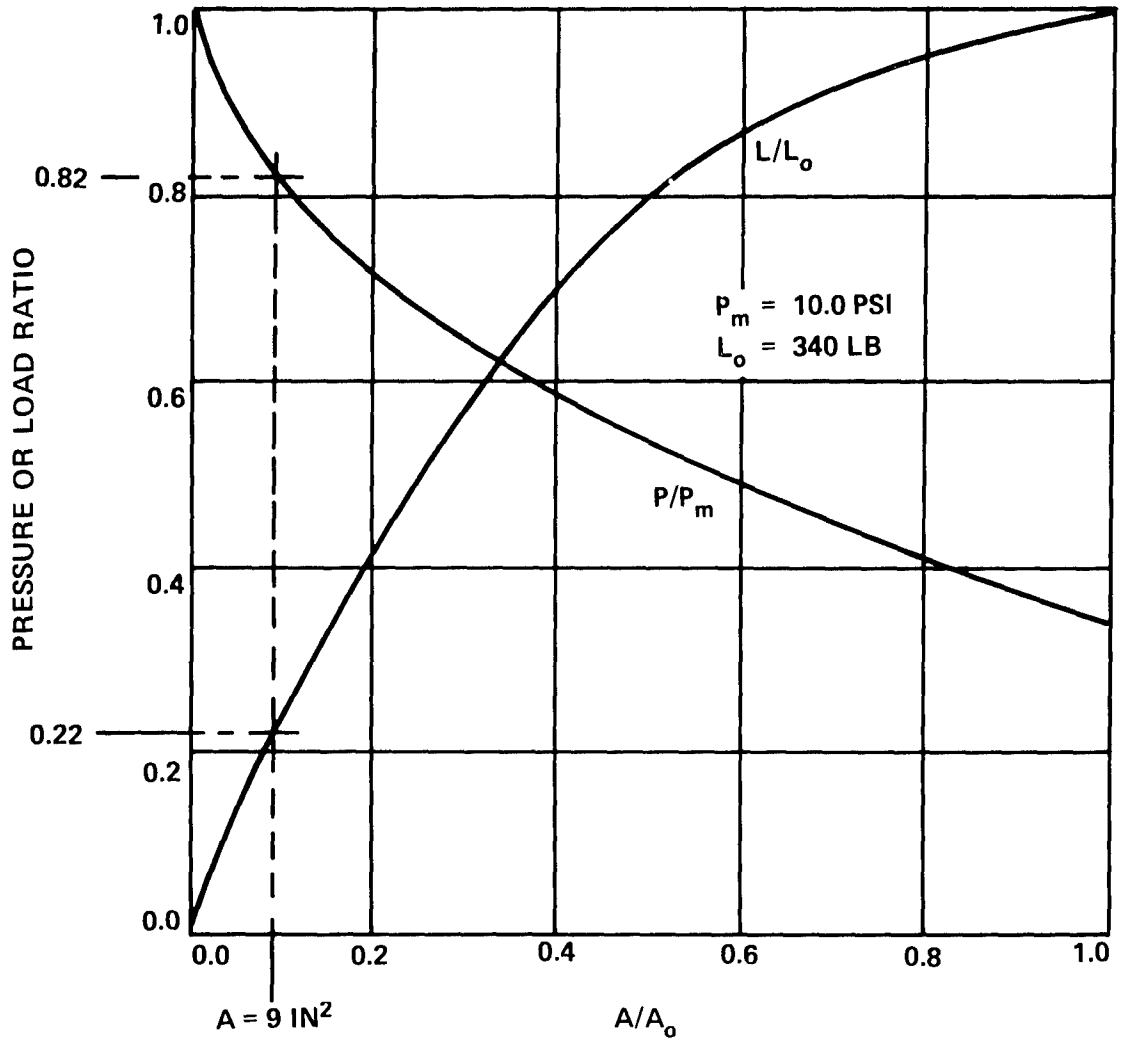

Figure C.2 - Normalized Pressure and Load versus Impact Area Relationships for the Isobaric Integration Example

APPENDIX D

SAMPLE PROBLEM

In order to demonstrate an application of the hull-water impact analysis computer program, it is used here to simulate an experimental run described by Chey[1] for the model shown in Figure 14. An explanation of the required input data and the resulting computer output is provided together with a sample of the computer output.

The run to be simulated consists of operating the varying-deadrise model at 30 ft/sec and 0-deg trim through a trochoidal wave with a length of 10 ft and a height of 9 in. Only one position is shown on the wave profile. It corresponds to the location of peak vertical and horizontal impact forces as determined by the computer program. Since only one location on the wave profile is considered, the data LAST is set equal to one.

Figure D.1 shows a profile of the varying-deadrise model. The model is partitioned into 32 incremental wedges, and 33 stations (N = 33) are used to define the necessary hull characteristic geometry. All but one of the wedges are 1 in. in length; the final bow wedge has a length of 0.5 in. The wedge density is, then, 1.0/31.5 = 0.0317 which satisfies the modeling technique requirement.

On the drawing, a "mean-chine line" is constructed which bisects the vertical line segment between chine and keel at each station. Although the chine does not extend to the bow, the mean-chine line is extended smoothly through the intersection of the keel and shear. Since it was decided to determine incremental wedge trim angles by using the mean-chine line, the datum IMCL is set equal to one.

The datum CONV is set equal to 1.0 because the offsets were not digitized. Instead, they were obtained directly from a drawing (3/8 in. = 1 in. scale). Therefore, the offsets listed in the output must be multiplied by the user-supplied scale factor which is the reciprocal of the drawing scale, or VNOC = 2.666.

The origin of the hull coordinate system is assumed to be at the step of the model, or XSTERN = 0.0. All of the required hull offsets are based on the hull coordinate system shown in Figure 14. As such, the first XKEEL value cooresponds to the location of XSTERN. The required hull offsets--XKEEL, YKEEL, YCHINE, ZKEEL, and ZCHINE--must then be defined for

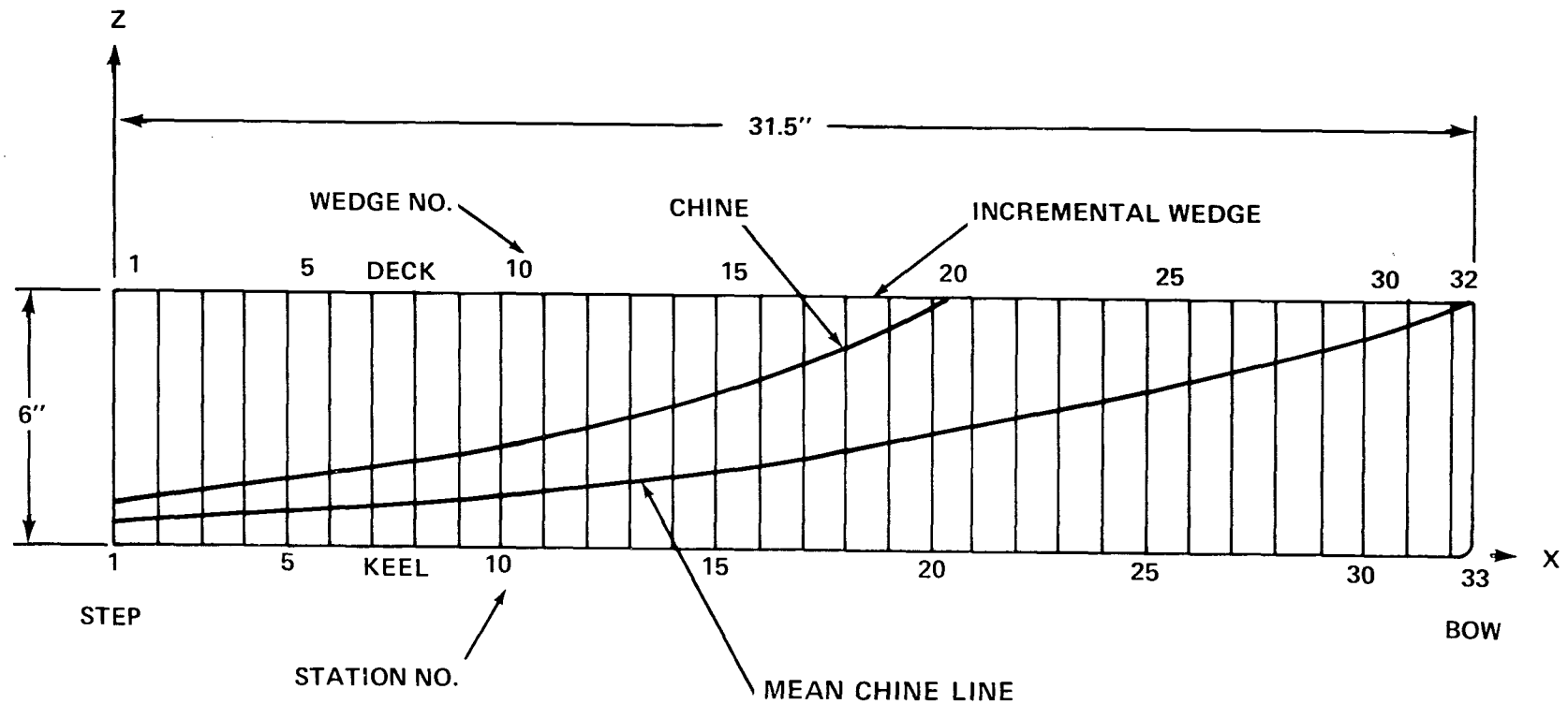

Figure D.1 - Incremental Wedge Approximation Method

each of the N stations. Since the datum IMCL was set equal to one, the Z-coordinates of the mean-chine line must also be defined for each of the N stations.

An arbitrary reference number of 3000 was chosen for ICASE. The Chey model tests[1] were conducted in a fresh-water tank; thus the datum IRHO is set equal to one. The rotation of the hull coordinate system, or the relative trim of the model TRIMD, is 0 deg. Since only one position on the wave profile and only one velocity condition are being simulated, both NPOS and NVELS are set equal to one.

The experimental run being considered involves hull-wave impacts; this requires that ICALM be equal to one so that the proper wave form may be defined. For this example, it is desired to demonstrate all forms of computer output. The output options were chosen accordingly, or IWRITE =1, IPG = 1, and ICURVE = 5. Input Cards 12 and 13 may then be omitted.

The trochoidal wave dimensions used for this example call for a wave length of 10 ft, WAVLEN = 120 in., and a wave height of 9.0 in., making AOVER2 = 4.5 in.

It is desired that transverse pressure distributions be calculated from Y/C = 0.0 to Y/C = 1.0 in increments of 0.05. This requires that for the input data, YRWO = YRDO = 0.0, YRWIN = YRDIN = 0.05, and YRWF = YRDF = 1.0.

The velocity input data are consistent with that specified by Chey.[1] As such, the horizontal velocity VELO is 360 in/sec and the vertical VELVER velocity is 0.0 in/sec. The pitch rate of the hull about its center of gravity OMEGA is 0.0 rad/sec. The datum XCG may then have any arbitrary value. Here, XCG is set equal to 0.0 in. forward of the step.

The hull position on the trochoidal wave profile is such that the wave crest is approximately concurrent with Station 23. This requires that the step, and in this case the origin of the hull coordinate system, be located 97.95 in. beyond the previous wave crest, or DELX = 97.95 in. Further, the step clearance above the mean waterline, which again corresponds to the origin of the hull coordinate system, must be 1.0 in. above the mean-water line, or DELZ = 1.0 in.

Figure D.2 is presented here to further explain the use of the mean-chine line. In the figure, a trochoidal wave profile is drawn to the same

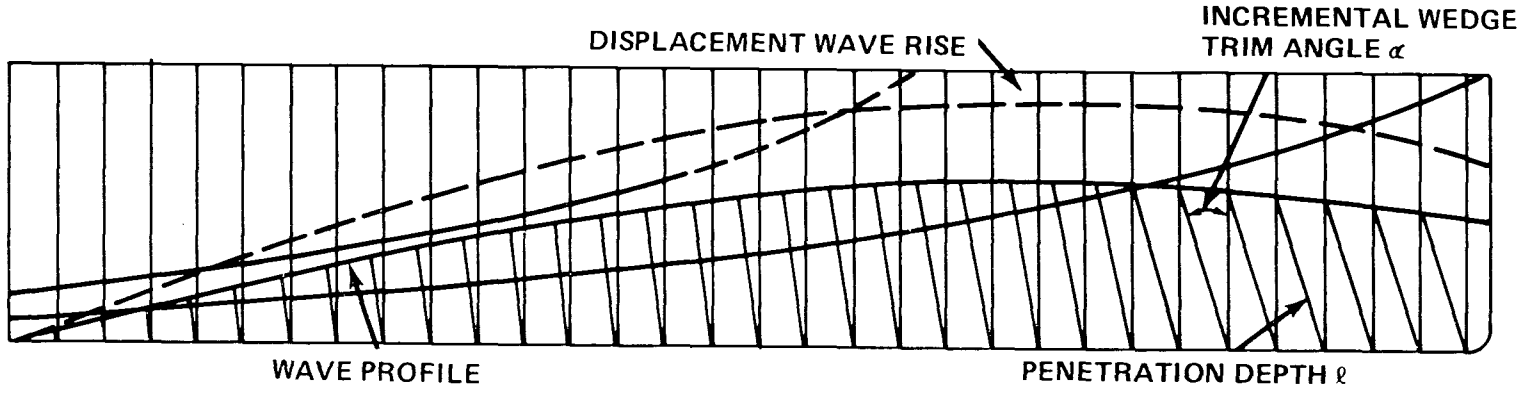

Figure D.2 - Hull-Wave Configuration

scale as the model and is overlaid at the desired position. A perpendicular to the mean-chine line is then erected from the intersection of the keel and station line at each of the N stations. The angle between this perpendicular and the station line is α_i, the local trim at that station. The penetration depth ℓ_i is measured along the perpendicular up to the water level indicated by the wave profile. Wedge parameters ℓ_i and α_i are determined by averaging the calculated parameters for each pair of boundary stations. If the constructed mean-chine line is approximately parallel to the keel, the penetration depths can be measured along a perpendicular to the keel, and the datum IMCL can be made greater than one.

Figure D.3 demonstrates the required control cards and input data. These data sufficiently defined the instantaneous impact condition. A quasi-static computerized analysis of the hull-wave impact was then performed.

The sample problem was run on the CDC 6700 by using a binary permanent file version of the computer program. It produced approximately 25 pages of output. The computer operating times for the sample problem were as follows:

CPA	096.338 sec
CPB	000.001 sec
PP	006.972 sec
IO	000.946 sec

Figure D.4 presents the normalized results of the analysis of pressure and load versus impact area. A partial listing of the output for that analysis is given as the final section of this appendix.

The analysis indicates that all of the incremental wedges were involved in the impact, making the wetted length of the hull equal to 31.492 in. It was found that a vertical force of 41.564 lb and a horizontal force of 7.663 lb acted on the hull as a result of the impact. These two forces may be interpreted as the impact lift and drag forces, respectively.

The maximum centerline pressure indicated 2.5582 psi on the first station of Wedge 32. However, the maximum detected pressure was found to be 4.7608 psi on the first station of Wedge 31. This is a "dry-chine" station, with the peak pressure occurring slightly inside the chine. The sample problem computer output includes transverse pressure distributions

```
CSRRABC,CM150000,T150,P3.                                    1735, RR JONES
CHARGE,CSRR,JOB NUMBER,PR,L.
ATTACH(IPPRES5,CSRRIPPRES5)
MAP,OFF.                                                     } CONTROL CARDS
SETCORE.
IPPRES5.
```

```
    1     HULL OF VARYING DEADRISE TEST CASES 17MAY72 ---------- CARD 1
   33          1          1.0          2.666 ---------- CARD 2
  0.0 ---------- CARD 3
  0.0       0.0       1.13       0.0        .4
 .3750      0.0       1.13       0.0       .450
 .7500      0.0       1.13       0.0       .500
1.125       0.0       1.13       0.0       .540
1.500       0.0       1.13       0.0       .600
1.875       0.0       1.13       0.0       .670
2.250       0.0       1.13       0.0       .720
2.625       0.0       1.13       0.0       .790
3.000       0.0       1.13       0.0       .860
3.375       0.0       1.13       0.0       .920
3.750       0.0       1.13       0.0       1.00
4.125       0.0       1.13       0.0       1.09
4.500       0.0       1.13       0.0       1.18
4.875       0.0       1.13       0.0       1.28
5.250       0.0       1.13       0.0       1.38
5.625       0.0       1.13       0.0       1.49
6.000       0.0       1.13       0.0       1.61      } CARD 4
6.375       0.0       1.13       0.0       1.75
6.750       0.0       1.13       0.0       1.91
7.125       0.0       1.13       0.0       2.10
7.500       0.0       1.08       0.0       2.24
7.875       0.0       0.99       0.0       2.24
8.250       0.0       0.90       0.0       2.24
8.625       0.0       0.81       0.0       2.24
9.000       0.0       0.72       0.0       2.24
9.375       0.0       0.63       0.0       2.24
9.750       0.0       0.54       0.0       2.24
10.125      0.0       0.45       0.0       2.24
10.50       0.0       0.36       0.0       2.24
10.875      0.0       0.27       0.0       2.24
11.25       0.0       0.18       0.0       2.24                CARD 5
11.625      0.0       0.09       0.0       2.24
11.8125     0.0       .0001      0.0       2.24
   .20      .22        .24        .26        .29       .32       .35       .38
   .42      .46        .50        .54        .58       .63       .68       .73
   .79      .85        .92        .99       1.06      1.13      1.21      1.30
  1.39     1.49       1.59       1.69       1.80      1.91      2.02      2.15
  2.24
  3000          1          0.0          1          1 ---------- CARD 6
     1          5            1          5 ---------- CARD 7
 120.0        4.5 ---------- CARD 8
   0.0        .05          1.0        0.0        .05       1.0 -- CARD 9
 360.0        0.0 ---------- CARD 10
   0.0        0.0 ---------- CARD 11
 97.95        1.0 ---------- CARD 14
```

Figure D.3 - Required Control Cards and Input Data for the Sample Problem

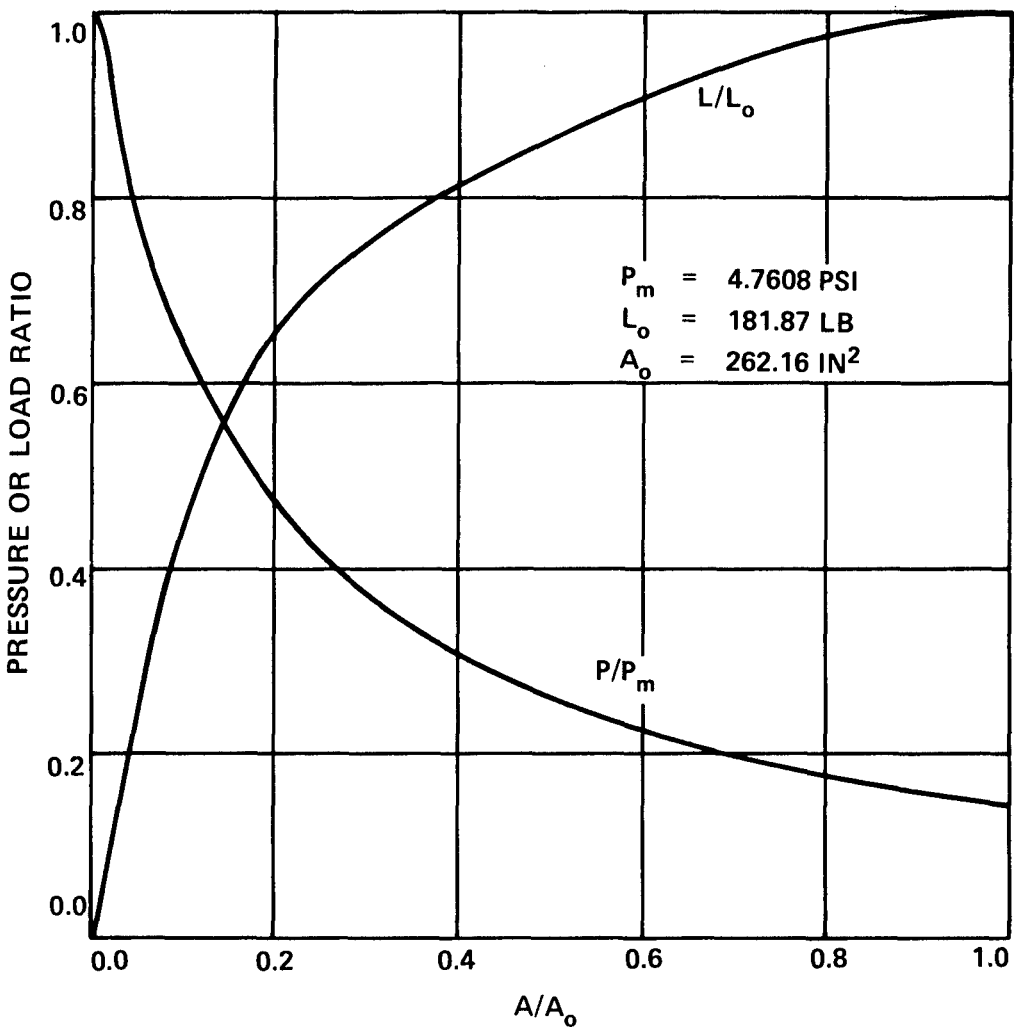

Figure D.4 - Normalized Pressure and Load versus Impact Area Relationships for the Sample Problem

only for Wedges 1, 2, 31, and 32. Wedges 3-30 were similarly printed out as requested by the input controls, but they are omitted here to minimize unnecessary repetition.

The contour integration routine analysis is summarized on the final page of the computer output. Since the impact is assumed to be bow-symmetric the tabulation provides pressure, load, and area relationships for only one side of the hull centerline. Both halves of the hull are assumed to behave identically. The analysis indicates that a normal impact load of 181.87 lb acted over 262.16 $in.^2$ of hull surface area. This area represents approximately 81 percent of the total possible load-bearing surface area, or the area defined by a shell expansion with the chine as the outer perimeter.

For a more in-depth explanation of the pressure distribution, see the column in the tabulation headed "Partial Impact Area." It shows that (40.04 + 55.15)/131.08 or approximately 72 percent of the wetted surface area had a pressure of less than 0.48 psi. Further, this area carried only about 27 percent of the total load or (4.77 + 24.46)/90.93. Finally, the average impact pressure acting on the hull is calculated as $0.146 \times 4.76 = 0.696$ psi.

The impact lift force obtained for this example was compared to the average amplitude of impact lift force as experimentally obtained by Chey.[1] The calculated, 41.564 lb and experimental, 56.0 lb, values differed by 25.8 percent. Likewise, the calculated drag, 7.663 lb, and the average amplitude of the impact drag, 15.5 lb, differed by 50.5 percent. Additional remarks on these results are included in the discussion of results. However, it should be noted that this correlation represents the largest discrepancy found between calculated and experimental results.

INPUT DATA DEFINITION

HULL OF VARYING DEADRISE TEST CASES 17MAY72

THE NUMBER OF HULL OPERATIONAL CONDITIONS BEING SIMULATED IS -- 1

N	IMCL	CONV	VNOC
33	1	1.000	2.666

XSTERN
0.00000

XKEEL	YKEEL	YCHINE	ZKEEL	ZCHINE
0.00000	0.00000	1.13000	0.00000	.40000
.37500	0.00000	1.13000	0.00000	.45000
.75000	0.00000	1.13000	0.00000	.50000
1.12500	0.00000	1.13000	0.00000	.54000
1.50000	0.00000	1.13000	0.00000	.60000
1.87500	0.00000	1.13000	0.00000	.67000
2.25000	0.00000	1.13000	0.00000	.72000
2.62500	0.00000	1.13000	0.00000	.79000
3.00000	0.00000	1.13000	0.00000	.86000
3.37500	0.00000	1.13000	0.00000	.92000
3.75000	0.00000	1.13000	0.00000	1.00000
4.12500	0.00000	1.13000	0.00000	1.09000
4.50000	0.00000	1.13000	0.00000	1.18000
4.87500	0.00000	1.13000	0.00000	1.28000
5.25000	0.00000	1.13000	0.00000	1.38000
5.62500	0.00000	1.13000	0.00000	1.49000
6.00000	0.00000	1.13000	0.00000	1.61000
6.37500	0.00000	1.13000	0.00000	1.75000
6.75000	0.00000	1.13000	0.00000	1.91000
7.12500	0.00000	1.13000	0.00000	2.10000
7.50000	0.00000	1.08000	0.00000	2.24000
7.87500	0.00000	.99000	0.00000	2.24000
8.25000	0.00000	.90000	0.00000	2.24000
8.62500	0.00000	.81000	0.00000	2.24000
9.00000	0.00000	.72000	0.00000	2.24000
9.37500	0.00000	.63000	0.00000	2.24000
9.75000	0.00000	.54000	0.00000	2.24000
10.12500	0.00000	.45000	0.00000	2.24000
10.50000	0.00000	.36000	0.00000	2.24000
10.87500	0.00000	.27000	0.00000	2.24000
11.25000	0.00000	.18000	0.00000	2.24000
11.62500	0.00000	.09000	0.00000	2.24000
11.81250	0.00000	.00010	0.00000	2.24000

ZMNCHL

.20000	.22000	.24000	.26000	.29000	.32000	.35000	.38000
.42000	.46000	.50000	.54000	.58000	.63000	.68000	.73000
.79000	.85000	.92000	.99000	1.06000	1.13000	1.21000	1.30000
1.39000	1.49000	1.59000	1.69000	1.80000	1.91000	2.02000	2.15000
2.24000							

WEDGE NO	AVERAGE BETA	CORRECTED BETA	ALPHA	TRIM ANGLE	WETTED LENGTH BEAMS	X/XMAX VARIES XRO	TO	XRF	IMMERSION DEPTH
1	20.6035	20.5767	3.05	3.053	.290	0.000		.032	.093
2	22.7911	22.7621	3.05	3.053	1.001	.032		.063	.311
3	24.7052	24.6743	3.05	3.053	1.860	.063		.095	.560
4	26.7546	26.6812	4.57	4.574	1.841	.095		.127	.803
5	29.3158	29.2379	4.57	4.574	2.476	.127		.159	1.042
6	31.5843	31.5028	4.57	4.574	3.147	.159		.190	1.276
7	33.7310	33.6466	4.57	4.574	3.851	.190		.222	1.503
8	36.1157	35.9615	6.09	6.089	3.440	.222		.254	1.720
9	38.2122	38.0548	6.09	6.089	4.025	.254		.286	1.930
10	40.3292	40.1694	6.09	6.089	4.643	.286		.317	2.132
11	42.7376	42.5761	6.09	6.089	5.296	.317		.349	2.323
12	45.1039	44.9418	6.09	6.089	5.984	.349		.381	2.503
13	47.4008	47.1491	7.59	7.595	5.369	.381		.413	2.670
14	49.6248	49.3755	7.59	7.595	5.988	.413		.444	2.825
15	51.7559	51.5102	7.59	7.595	6.649	.444		.476	2.967
16	53.8800	53.5346	9.09	9.090	6.132	.476		.508	3.096
17	56.0427	55.7064	9.09	9.090	6.770	.508		.540	3.211
18	58.2698	57.8292	10.57	10.574	6.399	.540		.571	3.313
19	60.5530	60.1311	10.57	10.574	7.049	.571		.603	3.398
20	62.9874	62.5884	10.57	10.574	7.938	.603		.635	3.464
21	65.2078	64.8322	10.57	10.574	9.352	.635		.667	3.517
22	67.1334	66.6733	12.04	12.043	9.940	.667		.698	3.561
23	69.1150	68.5751	13.50	13.496	10.882	.698		.730	3.591
24	71.1504	70.6544	13.50	13.496	13.626	.730		.762	3.600
25	73.2362	72.6849	14.93	14.931	15.718	.762		.794	3.592
26	75.3688	74.8806	14.93	14.931	20.738	.794		.825	3.560
27	77.5436	77.1225	14.93	14.931	28.562	.825		.857	3.510
28	79.7554	79.3334	16.35	16.348	38.124	.857		.889	3.450
29	81.9984	81.6659	16.35	16.348	61.438	.889		.921	3.363
30	84.2664	84.0265	16.35	16.348	116.969	.921		.952	3.267
31	86.5525	86.3517	19.12	19.120	270.894	.952		.984	3.219
32	88.8483	88.7225	25.64	25.641	1766.278	.984		1.000	3.233

```
CASE NUMBER =  3000 ,      POSITION NUMBER =      1
      THE HULL IS CONSIDERED TO BE OPERATING IN FRESH WATER.
      TRIM =    0.0000 DEGREES BY THE STERN
      WAVELENGTH X WAVE AMPLITUDE =     120.000 X       4.500 INCHES
      WET-CHINE INTEGRATION LIMITS =      0.0000      .0500     1.0000
      DRY-CHINE INTEGRATION LIMITS =      0.0000      .0500     1.0000
      SELECTED OUTPUT OPTIONS ARE --
           IWRITE =  1       IPG =  1       ICURVE =  5
      VERTICAL STEP LOCATION =       1.000 INCHES ABOVE MEAN-WATER LINE
      HORIZONTAL STEP LOCATION =      97.950 INCHES BEYOND WAVE CREST
      IMPACT OR PLANING OCCURS OVER WEDGES      1 TO     32
      TOTAL WETTED LENGTH =      31.492 INCHES
```

FOR VELOCITY CONDITION 1 THE VELOCITY COMPONENTS ARE --

HORIZONTAL = 360.000 INCHES/SECOND

VERTICAL = 0.000 INCHES/SECOND

PITCH = 0.000 RADIANS/SECOND

CENTER OF GRAVITY LOCATED 0.000 INCHES FORWARD OF THE STEP

WEDGE NUMBER	INCREMENTAL VERTICAL FORCES (LB)	INCREMENTAL HORIZONTAL FORCES (LB)	AVERAGE CENTERLINE PRESSURE (PSI)
1	.18	.01	.220
2	.58	.03	.223
3	.93	.05	.211
4	1.86	.15	.326
5	1.90	.15	.296
6	.89	.07	.205
7	.86	.07	.202
8	1.70	.18	.411
9	1.61	.17	.397
10	1.52	.16	.383
11	1.41	.15	.366
12	1.30	.14	.348
13	1.28	.17	.355
14	1.23	.16	.350
15	1.17	.16	.345
16	1.47	.24	.452
17	1.39	.22	.445
18	1.70	.32	.569
19	1.14	.21	.379
20	.84	.16	.284
21	.75	.14	.274
22	.84	.18	.337

23	.95	.23	.419
24	.91	.22	.441
25	1.03	.28	.561
26	.92	.25	.576
27	1.68	.45	.917
28	2.31	.68	1.292
29	2.51	.74	1.540
30	2.40	.70	1.798
31	1.99	.69	2.297
32	.31	.15	2.556

TOTAL VERTICAL FORCE= 41.564 POUNDS

TOTAL HORIZONTAL FORCE= 7.663 POUNDS

AVERAGE EQUIVALENT PLANING VELOCITY= 39.672 FEET PER SECOND

THE CENTERLINE PRESSURE ALONG THE HULL IS-

X/XMAX	P(PSI)	WET OR DRY CHINE
0.0000	.1776	DRY
.0159	.2300	DRY
.0317	.2513	DRY
.0317	.2115	DRY
.0476	.2232	DRY
.0635	.2329	DRY
.0635	.2041	DRY
.0794	.2109	DRY
.0952	.2167	DRY
.0952	.3194	DRY
.1111	.3259	DRY
.1270	.3316	DRY
.1270	.2919	DRY
.1429	.2964	DRY
.1587	.3004	DRY
.1587	.1956	WET
.1746	.2051	WET
.1905	.2140	WET
.1905	.1950	WET
.2063	.2026	WET
.2222	.2098	WET
.2222	.3978	WET
.2381	.4116	WET
.2540	.4248	WET
.2540	.3862	WET
.2698	.3976	WET
.2857	.4085	WET
.2857	.3741	WET
.3016	.3836	WET
.3175	.3925	WET
.3175	.3586	WET
.3333	.3663	WET
.3492	.3736	WET
.3492	.3423	WET
.3651	.3486	WET
.3810	.3545	WET
.3810	.3487	WET
.3968	.3553	WET
.4127	.3615	WET
.4127	.3442	WET
.4286	.3499	WET
.4444	.3554	WET
.4444	.3397	WET
.4603	.3448	WET
.4762	.3496	WET
.4762	.4450	WET
.4921	.4521	WET
.5079	.4591	WET
.5079	.4387	WET
.5238	.4452	WET
.5397	.4517	WET
.5397	.5596	WET
.5556	.5687	WET
.5714	.5779	WET
.5714	.5514	WET
.5873	.2907	DRY

.6032	.2950	DRY
.6032	.2800	DRY
.6190	.2841	DRY
.6349	.2884	DRY
.6349	.2699	DRY
.6508	.2740	DRY
.6667	.2782	DRY
.6667	.3312	DRY
.6825	.3371	DRY
.6984	.3433	DRY
.6984	.4055	DRY
.7143	.4188	DRY
.7302	.4336	DRY
.7302	.4253	DRY
.7460	.4406	DRY
.7619	.4569	DRY
.7619	.5419	DRY
.7778	.5604	DRY
.7937	.5803	DRY
.7937	.5567	DRY
.8095	.5756	DRY
.8254	.5957	DRY
.8254	.8994	DRY
.8413	.9166	DRY
.8571	.9348	DRY
.8571	1.2833	DRY
.8730	1.2923	DRY
.8889	1.3010	DRY
.8889	1.5373	DRY
.9048	1.5399	DRY
.9206	1.5418	DRY
.9206	1.7999	DRY
.9365	1.7981	DRY
.9524	1.7959	DRY
.9524	2.3012	DRY
.9683	2.2970	DRY
.9841	2.2926	DRY
.9841	2.5582	DRY
.9921	2.5556	DRY
1.0000	2.5530	DRY

NOTE- IN GENERAL, WET-CHINE TRANSVERSE DISTRIBUTIONS HAVE DECREASING VALUES OF PRESSURE IN THE CENTERLINE TO CHINE DIRECTION. DRY-CHINE DISTRIBUTIONS DISPLAY THE OPPOSITE TENDENCY.

NOW ALL THE WEDGES INVOLVED IN THE IMPACT OR PLANING AS DESIGNATED BY THE INPUT DATA ARE LISTED.

THE WEDGE NUMBER IS 1 FOR WHICH THE TRANSVERSE PRESSURE DISTRIBUTIONS ARE LISTED FOR X/XMAX VALUES OF-

Y/C	X/XM=0.0000 P(PSI)	X/XM= .0159 P(PSI)	X/XM= .0317 P(PSI)
0.0000	.1776	.2300	.2513
.0500	.1995	.2526	.2747
.1000	.3142	.3743	.4040
.1500	0.0000	0.0000	0.0000
.2000	0.0000	0.0000	0.0000
.2500	0.0000	0.0000	0.0000
.3000	0.0000	0.0000	0.0000
.3500	0.0000	0.0000	0.0000
.4000	0.0000	0.0000	0.0000
.4500	0.0000	0.0000	0.0000
.5000	0.0000	0.0000	0.0000
.5500	0.0000	0.0000	0.0000
.6000	0.0000	0.0000	0.0000
.6500	0.0000	0.0000	0.0000
.7000	0.0000	0.0000	0.0000
.7500	0.0000	0.0000	0.0000
.8000	0.0000	0.0000	0.0000
.8500	0.0000	0.0000	0.0000
.9000	0.0000	0.0000	0.0000
.9500	0.0000	0.0000	0.0000

THE WEDGE NUMBER IS 2 FOR WHICH THE TRANSVERSE PRESSURE DISTRIBUTIONS ARE LISTED FOR X/XMAX VALUES OF-

Y/C	X/XM= .0317 P(PSI)	X/XM= .0476 P(PSI)	X/XM= .0635 P(PSI)
0.0000	.2115	.2232	.2329
.0500	.2134	.2252	.2349
.1000	.2192	.2312	.2411
.1500	.2300	.2423	.2525
.2000	.2474	.2604	.2714
.2500	.2757	.2902	.3027
.3000	.3250	.3430	.3595
.3500	.4265	.4549	.4819

THE WEDGE NUMBER IS 31 FOR WHICH THE TRANSVERSE PRESSURE DISTRIBUTIONS ARE LISTED FOR X/XMAX VALUES OF-

Y/C	X/XM= .9524 P(PSI)	X/XM= .9683 P(PSI)	X/XM= .9841 P(PSI)
0.0000	2.3012	2.2970	2.2926
.0500	2.3045	2.3002	2.2957
.1000	2.3146	2.3098	2.3048
.1500	2.3315	2.3259	2.3202
.2000	2.3556	2.3489	2.3421
.2500	2.3874	2.3791	2.3709
.3000	2.4276	2.4173	2.4072
.3500	2.4769	2.4641	2.4516
.4000	2.5366	2.5205	2.5050
.4500	2.6081	2.5879	2.5688
.5000	2.6934	2.6681	2.6443
.5500	2.7951	2.7633	2.7336
.6000	2.9167	2.8766	2.8394
.6500	3.0631	3.0121	2.9652
.7000	3.2409	3.1754	3.1159
.7500	3.4598	3.3747	3.2983
.8000	3.7331	3.6212	3.5217
.8500	4.0781	3.9300	3.7992
.9000	4.4991	4.3147	4.1458
.9500	4.7608	4.7179	4.5544
1.0000	0.0000	3.6028	4.6849

THE WEDGE NUMBER IS 32 FOR WHICH THE TRANSVERSE PRESSURE DISTRIBUTIONS ARE LISTED FOR X/XMAX VALUES OF-

Y/C	X/XM= .9841 P(PSI)	X/XM= .9921 P(PSI)	X/XM=1.0000 P(PSI)
0.0000	2.5582	2.5556	2.5530
.0500	2.5612	2.5586	2.5559
.1000	2.5703	2.5674	2.5646
.1500	2.5855	2.5824	2.5791
.2000	2.6072	2.6035	2.5998
.2500	2.6356	2.6313	2.6269
.3000	2.6713	2.6660	2.6608
.3500	2.7146	2.7083	2.7020
.4000	2.7665	2.7588	2.7512
.4500	2.8277	2.8184	2.8092
.5000	2.8994	2.8881	2.8770
.5500	2.9827	2.9690	2.9556
.6000	3.0791	3.0625	3.0464
.6500	3.1899	3.1700	3.1506
.7000	3.3156	3.2920	3.2691
.7500	3.4541	3.4272	3.4009
.8000	3.5941	3.5670	3.5396
.8500	3.6913	3.6775	3.6591
.9000	3.5489	3.6177	3.6563
.9500	1.7934	2.5442	2.9853
1.0000	0.0000	0.0000	0.0000

THE MAXIMUM CALCULATED PRESSURE IS- 4.7608

PRESSURE AND LOAD VERSUS IMPACT AREA RATIO INFORMATION

PI MEAN CONTOUR PRESSURE (PSI)	AI PARTIAL IMPACT AREA (SQ.IN)	LI PARTIAL LOAD (LB)	SUM PARTIAL LOADS (LB)	SUM PARTIAL AREAS (SQ.IN)	A /AO IMPACT AREA RATIO	P /PM PRESSURE RATIO	L /LO LOAD RATIO
.12	40.04	4.77	90.93	131.08	1.000	.146	1.000
.36	55.15	19.69	86.17	91.04	.695	.199	.948
.60	6.08	3.62	66.48	35.89	.274	.389	.731
.83	4.21	3.51	62.86	29.81	.227	.443	.691
1.07	.35	.37	59.35	25.60	.195	.487	.653
1.31	4.68	6.13	58.98	25.25	.193	.491	.649
1.55	2.71	4.19	52.84	20.57	.157	.540	.581
1.79	3.44	6.14	48.65	17.86	.136	.572	.535
2.02	2.17	4.39	42.52	14.42	.110	.619	.468
2.26	2.04	4.61	38.13	12.25	.093	.654	.419
2.50	2.38	5.94	33.52	10.22	.078	.689	.369
2.74	1.88	5.13	27.58	7.84	.060	.739	.303
2.98	1.28	3.81	22.44	5.96	.045	.791	.247
3.21	1.08	3.46	18.63	4.68	.036	.836	.205
3.45	.60	2.08	15.17	3.60	.027	.884	.167
3.69	.58	2.15	13.09	3.00	.023	.916	.144
3.93	.21	.83	10.94	2.42	.018	.950	.120
4.17	.19	.79	10.10	2.21	.017	.962	.111
4.40	.19	.82	9.32	2.02	.015	.970	.102
4.64	1.83	8.50	8.50	1.83	.014	.975	.093

THE CALCULATED NORMAL IMPACT LOAD IS 181.87 POUNDS.

THE CALCULATED HULL IMPACT SURFACE AREA IS 262.16 SQUARE INCHES.

THE MAXIMUM DETECTED PRESSURE IS 4.76 PSI.

INITIAL DISTRIBUTION

Copies	
1	ARPA
1	DCS Logistics Dir, Transportation
1	Army Chief of R&D Combat Material Div
1	Army-Aviation Material Com
1	Army Combat Development Command, Ft. Belvoir CDC-MR-0
1	Army Combat Development Command Transportation Agency
1	Army Foreign Sci & Tech Center
1	Army Material RD&E Command
4	CHONR 1 ONR 439 1 ONR 461 1 ONR 463 1 ONR 480
1	NRL Tech Lib
1	DNL
1	USNA Lib
1	NAVPGSHCOL Lib (Code 0384)
1	USN ROTC, MIT
1	NAVWARCOL
9	NAVSHIPSYSCOM 1 SHIPS 031 1 SHIPS 034 2 SHIPS 034-12 1 SHIPS 0342 2 SHIPS 2052 2 PMS 382A
2	NAVAIRDEVCEN 1 Aero Str. Dept (Code ST) 1 Expl. Dev. (Code STD)

Copies	
1	NISC
9	NAVSEC 4 SEC 6110 1 SEC 6114D 1 SEC 6120 1 SEC 6128 1 SEC 6136
1	NAVAIRENGCEN
1	NAVAIRTESTCEN
12	DDC
1	Coast Guard, Ship Structures Comm
1	Library of Congress Science & Tech Div
2	MARAD 1 Ch Div of Ship Design 1 Office of R&D
1	NASA HQS Code RAA
1	National Science Foundation Engr Div
1	Dept of Transportation Office of Res & Tech
2	National Academy of Sciences 1 National Res Council 1 Ship Hull Res Comm
1	SNAME Slamming Panel
1	U Cal, Berkeley Dept of Naval Arch, Col of Eng
1	Catholic Univ Prof S. R. Heller, Jr.
1	MIT Dept of Ocean Eng
1	U of Mich Dept NAME
1	SWRI
1	SIT, Davidson Lab
1	American Bureau of Shipping S. G. Stiansen

CENTER DISTRIBUTION

Copies	Code	
1	11	
1	115	
1	1151	
1	1153	
1	1154	
1	1170	
1	1180	
1	1181	
1	1182	
1	15	
1	156	
1	16	
1	161	
1	163	
1	17	
1	1703	
1	172	
1	173	
1	1731	
28	1735	12 R.R. Jones 13 R.G. Allen
1	174	
1	1748	
1	177	
1	178	
1	27	
1	28	
1	9401	
1	9402	
1	9410	
3	9414	
1	9421	
1	9422	

Copies	Code
1	9423
5	9424
1	9427
2	9430
1	9431
1	9432
1	9440.1

UNCLASSIFIED
Security Classification

DOCUMENT CONTROL DATA - R & D

Security classification of title, body of abstract and indexing annotation must be entered when the overall report is classified)

1. ORIGINATING ACTIVITY (*Corporate author*)
Naval Ship Research and Development Center
Bethesda, Maryland 20034

2a. REPORT SECURITY CLASSIFICATION
UNCLASSIFIED

2b. GROUP

3. REPORT TITLE
A SEMIEMPIRICAL COMPUTERIZED METHOD FOR PREDICTING THREE-DIMENSIONAL HULL-WATER IMPACT PRESSURE DISTRIBUTIONS AND FORCES ON HIGH-PERFORMANCE HULLS

4. DESCRIPTIVE NOTES (*Type of report and inclusive dates*)

5. AUTHOR(S) (*First name, middle initial, last name*)
Robert R. Jones and Raymond G. Allen

6. REPORT DATE	7a. TOTAL NO. OF PAGES	7b. NO. OF REFS
December 1972	93	9

8a. CONTRACT OR GRANT NO	9a. ORIGINATOR'S REPORT NUMBER(S)
b. PROJECT NO	4005
c. In-house funding as authorized by SES Project Office letter F24:MEL:et of 11 August 1971 d.	9b. OTHER REPORT NO(S) (*Any other numbers that may be assigned this report*)

10. DISTRIBUTION STATEMENT
APPROVED FOR PUBLIC RELEASE: DISTRIBUTION UNLIMITED

11. SUPPLEMENTARY NOTES	12. SPONSORING MILITARY ACTIVITY
	SESPO (PM-17)

13. ABSTRACT

This report describes the development and usage of a semiempirical, quasi-static computerized method for calculating instantaneous three-dimensional water pressure distributions on high-speed marine vehicles. The method can simulate either planing or hull-wave impacts in three degrees of motion--pitch, heave, and surge. The analysis technique requires hull offsets, trochoidal wave parameters, and such initial condition information as the hull position, the vertical and horizontal velocity components, and the pitch rate. The method can be used to obtain results of varying complexity, including a description of normal pressures for all or selected portions of the hull, a normalized pressure versus impact area relationship, and horizontal and vertical impact forces. The results of its application to the analysis of the hull-wave impact of two model hull configurations are presented although the computer program developed for the method is not documented in this report.

14 KEY WORDS	LINK A		LINK B		LINK C	
	ROLE	WT	ROLE	WT	ROLE	WT
Three-Dimensional Pressure Distributions						
Impact						
Planing						
Prismatic Wedges						
Pressure-Load-Area Relationships						